Shales samples from the Chert-Spilite Formation in the Kinabalu area yielded Eocene and Lower Eocene faunas, while in the Segama Valley and Dervel Bay area (Fitch, 1955) and in the Kota Belud and Kudat area (Stephens, 1956) fossil assemblage from the Chert-Spilite Formation indicated a late Cretaceous to early Eocene age. Shale samples from the Trusmadi Formation were found to contain Eocene fossil assemblages, and one limestone sample indicated a Middle Eocene age.

Conglomerate containing Spilite was found associated with typical Trusmadi Formation rocks in Sungai Melaut by M. Bowen. Grit containing basalt was found as float in Sungai Kegibangan and appears to have been derived an area of Trusmadi Formation rocks. The extrusive rocks are presumably derived from the Chert-Spilite Formation, which would therefore be older than the Trusmadi Formation.

The Chert-Spilite Formation is generally cut by minor igneous intrusions, but no igneous intrusions have been found in the Trusmadi argillaceous rocks. This difference may be simply one of regional distribution; on the other hand, it may be due to the minor igneous intrusions being older than the Trusmadi rocks. It has sometimes been suggested that the quartz-veining which occurs commonly in the Trusmadi argillaceous rocks dates the strata as older than the other sedimentary rocks, including the Chert-Spilite Formation, in which quartz-veining is less widespread. However, it is not considered that this reasoning is valid, since the quartz-veining of the Trusmadi rocks does not seem to be due to hydrothermal deposition; no thick veins, zugs, or metalliferous minerals have been observed, and the veining is probably due to redeposition of quartz from sandstone and siltstone beds.

1-2-2 Igneous rocks

Igneous rocks occur only east of Sungai Kadamaian. Acid and ultrabasic rocks are the most important types, while intermediate and basic rocks are less common.

The largest igneous occurrence is Gunong Kinabalu, a large adamellite body from which the overlying and surrounding country rock has been eroded; associated minor intrusions occur around Kinabalu, particularly on the east. Surrounding mountain also, are ultrabasic bodies, older than the acid rocks. Small outcrops of andesite and rhyolite occur between Kinabalu and Paranchangan, and the basic rocks are

represented by small scattered occurrences of spilite, basalt, dolerite, and gabbro.

(1) Ultrabasic rocks

Ultrabasic phanerites occur over at least 100 square kilometers. Eight bodies are known; their locations are:

(a) Marai Parai:
A large ultrabasic body borders G. Kinabalu on the west, in the vicinity of a bare spur known as Marai parai.

(b) Kambaranga:
A long, narrow ultrabasic body forms the southern foot hills of G. Kinabalu.

(c) Pinosuk Plateau:
Small ultrabasic inliers protrude through the rock debris forming the Pinosuk Plateau.

(d) Sungai Lohan:
An irregular mass forming low hills occurs between Ranau and Hot Springs.

(e) Kampong Paring:
This ultrabasic body contains several small acid intrusions.

(f) Sungai Mankadau:
Ultrabasic rock forms a ridge appoximately 8 kilometers long on the north side of Sungai Mankadau.

(g) Sungai Meramuk:
The ultrabasic hills north of this river have a flat, and slightly inclined, surface, which is suggestive of a thrust plane.

(h) Kampong Tuhan:
Ultrabasic rocks occur about 3.2 kilometers south of Kampong Tuhan between Sungai Langanan and Sungai Mankadau.

Three of the masses (Kambaranga, Sungai Lohan, and Sungai Mankadau) are elongate in the sppoximate direction N100°E, which accords, although not perfectly,

with the regional trend of the surrounding sedimentary rocks, whose average strike direction in N120°E, the other bodies are irregular and do not appear to have a predominant axis.

The ultrabasic rocks comprise dunite, harzburgite, hornblende peridotite, and serpentine, which occur together in the various bodies.

The freshly exposed ultrabasic rock is dark blue, often with a rather greenish waxy appearance; on weathering the rock develops a thin skin, usually less than half an inch thick, which is hard and rough and rust-brown.

The ultrabasic rocks are resistant to weathering, and there is almost no intermediate stage between fresh rock and completely altered clay; there is no thick zone of soft decayed material, such as is found on sandstone or more acid igneous rocks. Thus the depth of weathering on the ultrabasic rocks is not deep, and outcrops are common in rivers. The effect of the shallow weathering is shown by the frequent occurrence of boulders on hillsides. The colour of the soil is distinctive, being bright red-brown when freshly cut and slowly becoming a less bright rust colour after long exposure.

(2) Basic intrusive rock

Basic igneous intrusive rock lies 8 kilometers east of Ranau in steep hilly country rising to about 900 meters between the Paginatan bridle path and Sungai Liwagu; the most prominent hill is Bukit Morouporou. The body consists mainly of gabbro, often sheared and altered, with small amounts of ultrabasic rock. The area, covering about 30 square kilometers, may be useful for agricultural purpose as the soil appears to be deep and to have good structure.

(3) Acid phanerites

The Gunong Kinabalu intrusion is a pluton mainly of hornblende adamellite that was emplaced diapirically into the complex of older rocks. It is part of a large batholith underlying the area, and was emplaced 9 million years ago. The central part of the batholith was probably uplifted by faulting in the lower Pleistcene to form the present mountain.

Jointing in the Kinabalu body can be seen in the air photographs, and the joint

pattern is roughly radial, the focus being approximately in the center of the mountain. At north end of the western limb, there is pronounced vertical 'platy' structure, the direction of the plates being approximately N120°E, similar structure can be seen at the southeast of the eastern limb, and here the trend of the plates varies from N10°W to N20°E. Between these two areas jointing is not so pronounced. Southeast of Low's Peak, the direction of jointing is approximately N80°E which accords with the principal direction of the aplites at that place.

The acid phanerites are mainly adamellite and granodiorite, while monzonite and granite occur less frequently; associated fine-grained rocks are microadamellite and micromonzonite. Adamellite is the most common rock type; it is a medium-to coarse-grained leucocratic rock, consisting of euhedral hornblende (20 percent), plagioclase (30 percent), anhedral orthoclase (40 percent), and quartz (10 percent); the percentages are estimated from a typical sample. Biotite is rare, and the principal accessory minerals are magnetite and pyrite. Large phenocrysts of orthoclase, up to 4 centimeters long, occur in some specimens, epecially those from boulders in Sungai Kadamaian and its tributaries. The other rock types consist of the same minerals, and differ only in the proportions contained.

The acid phanerites are younger than the ultrabasic, and this is clearly demonstrated in Sungai Meramuk. The river runs approximately along a junction of peridotite and monzonite, where small xenoliths of the former occur in the latter. Xenoliths of sedimentary rock also occur there; some are only partially altered and still show some bedding, while others are so far recrystallised that they appear as dark fine-grained crystalline enclaves in the monzonite.

(4) Acid and intermediate aphanites

Acid and intermediate aphanites occur east of Gunong Kinabalu:

(a) Bukit Kotud and adjacent hills:

Between Sungai Mankadau and Sungai Langanan there are four small conical hills; two of these, Bukit Kotud and Bukit Tambian, are known to be stocks of andesite, while the other two, Bukit Pu'us and Bukit Kalarakan, resemble them morphologically and are probably also andesite stocks.

(b) Bukit Luminantai-Bukit Kimundu area

Microgranodiorite intrusions occur at Bt. Kimundu, Bt. Kiapako, Bt. Luminantai, and Bt. Dumarun. Hornblende microgranodiorite intrusives forming Bt. Kimundu and Bt. Kiapako intrude into the Trusmadi Formation which consists of broken sandstone beds in highly sheared black shaly matrix and medium-grained porphyritic, grey hornblende microgranodiorite intrusion forming Bt. Luminantai, Bt. Dumarun, and adjacent hills intrudes into siltstone, sandstone, grey and red shale of the Crocker Formation. The contacts between the sedimentary rocks and microgranodiorite are sharp and the intruded rocks are slightly metamorphosed.

(5) Aplites in the Kinabalu intrusion

Aplites are common in the Kinabalu intrusion, but they are rare in the country rock and infrequent in the other acid plutonic intrusions. Aplite veins vary in thickness from about 5 centimeters to over 60 centimeters and have a sharp margin with the surrounding igneous rock. It is clear that the aplites were emplaced as a magma, probably along joints, and that they are not of the metasomatic type.

The aplite veins are especially common on the summit plateau of Kinabalu, and they can be clearly traced for many meters across the bare rock; the directions vary, but observations made southeast of low's Peak show that the dominant direction there is N80°E; out of 19 veins measured, 11 trended in this direction, and this conforms to what is believed to be the direction of jointing there.

(6) Pegmatite and aplite in ultrabasic rocks

A pegmatite and several aplites have been found intrusive into ultrabasic rock near Paranchangan. The only acid rocks exposed from which these veins could have been derives are the Kinabalu granodiorite and associated minor intrusions.

The pegmatite, found by N. Wong in 1957, is about 1,200 meters northeast of Paranchangan, close to the chromite deposit. The outcrop is about 30 meters by 60 meters, roughly oval in outline, and entirely surrounded by ultrabasic rock. The pegmatite is marked by superficial blocks of coarse quartz and felspar with occasional 'books' of muscovite, and small hornblende crystals.

Aplite blocks occur on the tract from Panugaran to Tagis at three places; the rock has not been seen in situ, but the blocks are probably more or less in place. The occurrences are entirely surrounded by ultrabasic rock.

1-2-3 Structure

There are two dominant directions of folding in the sedimentary rocks from the coast almost to Sungai Kadamaian, the axis is northeast, with a predominant dip southeast, while further inland, the rocks are folded on an east-southeast axis, with the majority of the dips to the south-southwest. It is probable that, while they are all Eocene, the rocks east of the Kadamaian are older than those on the west, and that the two formations have been subject to different tectonic conditions. Overfolding has been observed between Togop and Kelawat; this, with the predominence of dips to the southeast and scarcity of northwest dips, suggests that the crocker Range may be isoclinally folded. (compiled from Collenette, P., 1954 and 1957, Jacobson, G., 1970)

Table II-1-2 Stratigraphy of the Kinabalu Region

AGE	TERTIARY LETTER CLASSIFICATION	SEDIMENTARY ROCKS	IGNEOUS ROCKS	ABSOLUTE AGE m.y.	PALAEOGEOGRAPHY AND DIASTROPHISM
HOLOCENE		RECENT ALLUVIUM : boulder gravel			Erosion
PLEISTOCENE	Th	PINOSUK GRAVELS clayey to sandy boulder gravel	Uplift of Kinabalu pluton	15	Glacial and periglacial erosion and re-deposition Uplift and differential warping
PLIOCENE	Tg	Non-deposition			Peneplanation
MIOCENE	Tf		Intrusion of the Kinabalu batholith : mainly adamellite	7 9	
		(WARIU FORMATION : slump breccia)			Gravity sliding and slumping following uplift
	Te_5	Non-deposition	Emplacement of ultrabasic rocks by faulting		Strong folding, faulting, and uplift
OLIGOCENE	Te_{1-4}	CROCKER FORMATION : sandstone, siltstone, red and grey shale and mudstone		26	Infilling of eugeosynclinal trough
	Tcd			38	
EOCENE	Tb	TRUSMADI FORMATION : grey and dark grey argillite, slate, siltstone and sandstone	Intermittent spilite lavas		Eugeosynclinal, flysch-type deposition
PALAEOCENE	Ta			54	
UPPER CRETACEOUS		(CHERT-SPILITE FORMATION : chert, greywacke, limestone)	(Basic intrusive and extrusive rocks : mainly spilite and sodic dolerite)	65	
			Intrusion of ultrabasic rocks at depth	100	Initiation of eugeosynclinal trough
LOWER CRETACEOUS		Non-deposition			
TRIASSIC-JURASSIC OR OLDER		CRYSTALLINE BASEMENT : schist, gneiss		136	Deposition, folding, and metamorphism of the Crystalline Basement. Possibly two cycles of intrusion

(taken from Jacobson, G., 1970)

1-3 Result of the Survey

1-3-1 Investigation of Locality of Mineral Occurrence

Twelve localities of mineral occurrence in total, namely four localities of epithermal (gold)-pyrite-limonite-bearing quartz veinlets in hydrothermally altered acidic to intermediate volcanic and pyroclastic rocks, which appear to be of Miocene to Pliocene age, around Bt. Tampang, two localities of limonite·quartz network and limonite network in quartz monzonite porphyry around Bt. Luminantai, four localities of limonite-bearing quartz veins embedded in faults in the alternating beds of sandstone and shale (sandstone ≫ shale) of Trusmadi Formation of Paleocene to Eocene age in the Kg. Randagong area, one locality, which is found in the old adit in the Pingan Pingan area, of Cyprus type cupriferous iron sulfide network embedded in pillow basalt of the ophiolite complex, one locality of floats of Cyprus type massive cupriferous iron sulfide found in S. Lingangah, a tributary on the northern side of S. Mankadau, were investigated.

The result of the investigation is summarized in the Table II-1-3 and the location of locality of mineral occurrence is shown in the Fig. II-1-1 and Fig. II-1-2 attached at the end of this report.

The results of the chemical analysis and microscopic observation of ore samples taken at the localities of mineral occurrence are given in the Table II-1-9 in the following section 1-4 and in the Table II-1-7 in the section 1-3-2-(5) respectively.

The results of the chemical analysis and microscopic observation of the representative rock samples taken at and around the localities of mineral occurrence are given in the Table II-1-5 in the following section 1-3-2-(2) and in the Table II-1-6 in the section 1-3-2-(3) respectively.

The result of the X-ray diffraction examination of hydrothermally altered rock taken in the Bt. Tampang and Bt. Luminantai areas is shown in the Table II-1-8 in the section 1-3-2-(6) and the homogenization temperature of fluid inclusions in quartz taken from pyrite-limonite-bearing quartz veinlets embedded in hydrothermally altered rock in Bt. Tampang area, from limonite·quartz veinlets in hydrothermal alteration vein in the Bt. Luminantai area, and from limonite-bearing quartz veins in the Kg. Randagong area, is given in the histgrams of the Fig. II-1-12, II-1-13, and II-1-14 in the section 1-3-2-(7) respectively.

The result of the investigation of the main localities of mineral occurrence is summarized below.

(1) Bt. Tampang area

The mineralized zone of veinlet (1 ~ 10 cm wide), network, or dissemination, consisting of quartz with minor amounts of pyrite and limonite, embedded in acidic to intermediate volcanic and pyroclastic rocks subjected to hydrothermal alteration (silicification, sericitization, kaolinitization, chloritization, and local montmorillonitization) is found at the western and southern foots of Bt. Tampang. Geology along a road at the western foot of Bt. Tampang is shown in the Fig. II-1-6 attached at the end of this report.

The assay result of five ore samples taken at these localities of mineral occurrence reveals that the sample T-10-0 contains 2.68 g/t of gold and T-1-0-2 contains 0.16% of lead and 22.05 ppm of mercury and that 0.13% of antimony and 22.45 ppm of mercury are contained in the samples T-1-0-1 and T-3-0 respectively. It is generally said that minor elements such as mercury and antimony together with arsenic are found at the upper part of the gold deposit.

The result of the X-ray diffraction examination of 12 samples taken from acidic to intermediate volcanic and pyroclastic rocks and sedimentary rock subjected to hydrothermal alteration reveals that the hydrothermal alteration zone around Bt. Tampang consists mainly of a large quantity of quartz, a minor amount to a trace of kaolinite, a trace of chlorite, and a trace of sericite and contains, in places, a middle to small quantity of potash felspar and a trace of smectite in addition to the above four minerals.

The mineral assemblage of the hydrothermal alteration zone is similar to that of the upper part of the hydrothermal alteration zone formed by intermediate to weak alkaline hydrothermal liquid accompanying epithermal gold deposit of the adularia-sericite type (Hayba et al., 1986; Heald et al., 1987) or of the low sulfidation system (Hedenquist, 1987), or is similar to that of the hydrothermal alteration zone, ranging from the lower mica-chlorite zone to the upper kaolinite-mica zone, accompanying epithermal gold deposits in Kyushu of Japan (Izawa, 1988).

As the result of the measurement of the homogenization temperature of the fluid inclusions in four quartz samples taken from (gold)-pyrite-limonite-bearing quartz veins in the hydrothermal alteration zone, temperatures of 219° to 237°C (average 228°C), 218° to 256°C (average 237°C), 232° to 259°C (average 248°C), and 278° to 284°C (average 281°C) have been obtained. The homogenization temperature of 218° to 284°C obtained from four quartz samples is included in the range of 200° to 300°C of high sulfidation system epithermal gold deposit (Hedenquist, 1987) accompanying hydrothermal liquid

related to the volcanic activity in the Circum-Pacific region, rather than the range of 170° to 270°C of the low sulfidation system, or is included in the range of 133° to 349°C of the adularia-sericite type or in the range of 120° to 320°C of the acid-sulfate type gold deposit in the western Pacific island arcs region. (Sillitoe, 1988)

(2) Bt. Luminantai area

The veined hydrothermal alteration zones accompanied locally by limonite and quartz are found along many parallel joints in quartz monzonite porphyry around Bt. Luminantai. Hydrothermal alteration veins are narrow in width and 1 to 30 centimeters wide. At the Lu-2 locality of mineral occurrence, 35 hydrothermal alteration veins are found along roughly parallel joints (strike: E-W, dip: 90°) for a distance of 17 meters, and at the Lu-3 locality, 46 hydrothermal alteration veins are exposed along roughly parallel joints (strike: N60°W, dip: 90°) for a distance of 40 meters. The both hydrothermal alteration veins at Lu-2 and Lu-3 localities form respectively network as a whole. However, no massive hydrothermal alteration zone is found, because quartz monzonite porphyry between hydrothermal alteration veins has not been subjected to hydrothermal alteration.

The assay result of two samples taken from hydrothermal alteration veins rich in quartz and limonite at Lu-2 and Lu-3 localities reveals that the sample Lu-2-0 contains 2.46% of Pb, 0.13% of Zn, 0.10% of Cu, 11.1 g/t of Ag, and 0.10 g/t of Au.

The result of the X-ray diffraction examination of three samples (Lu-2-X, Lu-3-X) taken from hydrothermal alteration veins at Lu-2, Lu-3, and Lu-5 localities reveals that these hydrothermal alteration veins consist mainly of a large quantity of quartz, a trace of chlorite and kaolinite, a middle quantity to a trace of potash felspar, and a minor amount to a trace of sericite, and contain a trace of montmorillonite locally in addition to the above five minerals. The mineral assemblage of hydrothermal alteration veins is similar to that of the SCC zone (sericite, clay, chlorite), proposed by Sillitoe et al. (1984), accompanying the upper part of porphyry copper deposit in the Philippines.

The measurement of the homogenization temperature of the fluid inclusions in quartz taken from limonite-bearing quartz veinlet in hydrothermal alteration vein at the Lu-3 locality reveals that the homogenization temperature ranges from 350° to 417°C (average 384°C) and is included in the range of that of quartz vein accompanying porphyry copper deposit (300° to 480°C in case of

Mamut deposit; after Nagano et al., 1977). However, owing to a lack of the number of the sample, a definite conclusion about the above must be reserved.

(3) Kg. Randagong area

Four outcrops (R-1, R-2, R-3, R-5) of limonite-bearing quartz veins embedded in faults in the alternating beds of sandstone and shale (sandstone ≫ shale) of Trusmadi Formation of Paleocene to Eocene age and floats of high grade stibnite ore are found in the Samalang river basin in the Kg. Randagong area.
Thinking that limonite accomanying quartz veins found at four outcrops might be formed by oxidation of stibnite, four samples of limonite-bearing quartz veins (R-1-0, R-2-0, R-3-0, R-5-0-1) were assayed. However, the assay result reveals that no useful metal including antimony is contained in the samples, while a float of high grade ore of stibnite (R-5-0-2) taken at the dry riverbed of the S. Samalang close to the outcrop of the R-5 locality contains 23.79% of Sb.

(4) Kg. Pingan Pingan area

The mineralized zone of Cyprus type networked and disseminated cupriferous iron sulfide in pillow basat of the ophiolite complex is found in the old adit (PP-2 locality) about two kilometers east of Kg. Pingan Pingan situated along Marudu Bay in northern Sabah.
The mineralized zone of networked and disseminated iron sulfide consisting of pyrite with a trace of sphalerite and malachite is three meters wide and trends in a north-south direction.
The assay result reveals that the sample of networked and disseminated ore (PP-2-0) taken in the old adit contains 0.62% of Zn as useful metal.
Trenching had been carried out at the surface to the north of the old adit by Mamut Copper Mining Adn. Bhd. (MCM). However, it was not able to confirm the result of the trenching at the time of the investigation, because all the trenches were restored by the reclamation.

Table II-1-3 List of Localities of Mineral Occurrence Investigated in Kinabalu Region

Region	Locality Name	Locality Number	Mineral Assemblage	Occurrence	Strike & Dip	Size of Orebody (in meter)	Host Rock	Alteration of Host Rock	Sample No.
Kinabalu	Lingangah	L-1*	Py·cp·bo·hm·lim+mal	boulder of massive ore	—	max. 3.0×1.3×1.3	—	—	L-1-0
"	Luminantai	Lu-2	lim·gn	network	E-W·90°	L=6.0+, W=17.0	guartz monzonite porphyry	silicification, kaolinization chloritization, sericitization	Lu-2-0
"	"	Lu-3	lim·qz	network	N60°W·90°	L=6.0+, W=40.0	guartz monzonite porpluyry	silicification, chloritization, sericitization, kaolinization	Lu-3-0
"	Pingan Pingan	PP-2	lim·py·qz+mal	network	N-S·90°	L=5.0+, W=3.0	pillow basalt	chloritization, silicification, epidotization	PP-2-0
"	Randagong	R-1	qz·lim	vein along fault	N86°W·48°N	L=2.7, W=0.05~0.14	sandstone, shale	none	R-1-0
"	"	R-2	qz+lim	vein along fault	N60°W·70°N	H=2.0+, W=2.0	sandstone, shale	none	R-2-0
"	"	R-3	qz+lim	vein along fault	N3°W·70°W	L=1.0, W=0.1~0.15	sandstone, shale	none	R-3-0
"	"	R-5	sb·qz·py	vein along fault	N14°E·70°W	L=3.0+,H=2.0,W=0.25	sandstone, shale	none	R-5-0-1
"	Tampang	T-1	qz+py·lim	network	N45°W·86°N	H=2.0+, W=1.0	dacitic tuff breccia	silicification, sericitization, kaolinization, chloritization	T-1-0-1 T-1-0-2
"	"	T-3	qz+lim·py	lenticular	—	L=0.25, W=0.1	rhyolitic tuff breccia	silicification, sericitization, kaolinization, chloritization	T-3-0
"	"	T-7	py·lim	disseminated~lenticular	—	L=0.3, W=0.15	trachytic tuff breccia	silicification, sericitization, kaolinization, chloritization	T-7-0
"	"	T-10	qz+lim	vein along joint	N20°E·80°W	L=0.8, W=0.01~0.15	tuff	silicification, chloritization, sericitization, kaolinization, montmorillonitization	T-10-0

Abbreviations:
*: boulder of gossan, py: pyrite, cp: chalcopyrite, bo: bornite, hm: hematite, lim: limonite, mal: malachite, qz: quartz, sb: stibnite, gn: galena, max.: maximum, L: length, W: width, H: height, 6.0+: 6.0 and over

1-3-2 Laboratory Work

(1) K-Ar age determination of rock (9 samples)

Nine representative rock samples, namely 3 samples (Km-1-D, K-1-D, Lu-1-D) taken from acidic intrusive rock which are found between Bt. Kimudu and Bt. Kamunsu, 2 samples (S-1-D, Ma-2-D) from intermediate intrusive rocks to the west of Kg. Merungin, 2 samples (M-1-D, PP-2-D) of basalt and 1 sample (Mo-1-D) of gabbro in the ophiolite complex, and 1 sample (T-4-D) of sandstone taken at the foot of Bt. Tampang, out of 18 rock samples taken at and near the localities of mineral occurrence for the microscopic observation and chemical analysis, were dated by means of the K-Ar method of whole rock.

The result is shown in the Table II-1-4. As shown in the Table II-1-4, five samples of acidic and intermediate intrusive rocks have been dated as 6.85±0.17 to 7.47±0.20 Ma (Late Miocene). The ages of two samples of basalt (M-1-D, PP-2-D) and one sample of gabbro (Mo-1-D) in the ophiolite complex have been determined as 17.0±0.65 Ma (Middle Miocene), 44.9±9.3 Ma (Middle Eocene), and 57.0±11.45 Ma (Late Paleocene) on the average respectively. The age of 70.8±2.2 Ma (Late Cretaceous) on the average has been obtained from sandstone (T-4-D) taken at the foot of Bt. Tampang.

Table II-1-4 Result of K-Ar Dating of Rock Samples in Kinabalu Region

Locality Name	Sample Number	Numbers in Laboratory	Sample Type	Potassium (K wt%)	Rad. ^{40}Ar (10^{-8}cc/g)	K-Ar Age (Ma)	Air Cont. (%)
Kamunsu	Km-1-D	SH5-208 -209	Whole Rock (Granodiorite porphyry)	2.36 ±0.05	67.0±1.2 68.4±1.2	7.32±0.20 7.47±0.20 Avg. 7.39±0.20	39.6 38.4
Kiapako	K-1-D	SH5-210 -211	Whole Rock (Quartz diorite porphry)	3.31 ±0.07	88.3±1.3 88.1±1.3	6.87±0.17 6.85±0.17 Avg. 6.86±0.17	29.2 28.6
Luminantai	Lu-1-D	SH5-212 -213	Whole Rock (Quartz monzonite porphyry)	3.21 ±0.60	90.0±1.1 89.7±1.1	7.21±0.17 7.19±0.17 Avg. 7.20±0.17	14.8 14.9
Mankadau	M-1-D	SH5-204 -223	Whole Rock (Basalt)	1.27 ±0.04	84.1±2.1 83.3±1.4	17.1±0.7 16.9±0.6 Avg. 17.0±0.65	29.5 34.6
Morouporou	Mo-1-D	SH5-218 -219	Whole Rock (Gabbro)	0.13 ±0.03	29.6±1.1 28.8±1.1	57.8±11.6 56.2±11.3 Avg. 57.0±11.45	65.9 66.4
Pingan Pingan	PP-2-D	SH5-220 -221	Whole Rock (Basalt)	0.07 ±0.01	12.3±0.8 12.4±0.8	44.8±9.3 45.0±9.3 Avg. 44.9±9.3	78.9 78.7
Sasapan	S-1-D	SH5-214 -215	Whole Rock (Diorite porphyrite)	2.26 ±0.05	65.1±0.9 64.0±0.8	7.42±0.18 7.31±0.17 Avg. 7.36±0.17	20.7 20.4
Tagap	Ta-2-D	SH5-216 -217	Whole Rock (Diorite porphyrite)	2.31 ±0.05	66.2±2.6 66.5±2.6	7.38±0.32 7.42±0.33 Avg. 7.40±0.32	68.2 68.6
Tampang	T-4-D	SH5-224 -225	Whole Rock (Sandstone)	1.02 ±0.03	284±3 285±3	70.6±2.2 71.0±2.2 Avg. 70.8±2.2	11.5 11.6

(2) Chemical analysis of rock (18 samples)

The assay result of 18 rock samples, namely 9 samples taken at the same localities as the samples for the K-Ar age determination, 2 samples of acidic itrusive rock around Bt. Luminantai, 3 samples of ultrabasic rock and 1 sample of basalt in the ophiolite complex, 1 sample of dacite, 1 sample of rhyolite, and 1 sample of trachytic tuff around Bt. Tampang, is shown in the Table II-1-5. The analyses of 8 samples, namely 3 samples (M-1-R, PP-1-R, PP-2-R) of basalt of the ophiolite complex, 2 samples (S-1-R, Ta-2-R) of diorite porphyrite in the Kg. Merungin area, 1 sample (T-3-R) of rhyolite, 1 sample (T-1-R) of dacite and 1 sample (T-7-R) of trachytic tuff around Bt. Tampang, out of 18 rock samples analyzed chemically, have been plotted on the following several diagrams for the petrological study.

At first, the analyses of SiO_2 and Na_2O+K_2O have been plotted on the SiO_2-Na_2O+K_2O diagram and the result is given in the Fig. II-1-7. The Fig. II-1-7 shows that three basalts have been plotted within the fields of alkali basalt and high alkali tholeiite series after Kuno (1968), with two diorite porphyrites in the high alkali tholeiite series roughly and three volcanic and pyroclastic rocks in the high alkali tholeiite and low alkali tholeiite series.

Secondly, the MFA trigonal diagram of the Fig. II-1-8, on which the analyses of MgO, Na_2O+K_2O, and FeO* calculated as total FeO from the analyses of FeO and Fe_2O_3 have been plotted, indicates that the sample PP-1-R (basalt) and T-7-R (trachytic tuff) have been plotted in the field of the tholeiite series after Irvine and Barager (1971) and T-3-R (rhyolite) has been plotted around the boundary between the tholeiite and calc-alkali rock series with the remaining five samples in the calc-alkali rock series.

Thirdly, the SiO_2-FeO*/MgO diagram of the Fig. II-1-9 shows that the sample T-3-R (rhyolite), which has been plotted in the field of the tholeiite series out of the diagram due to high FeO*/MgO value of 11.30, T-7-R (trachytic tuff), and M-1-R (basalt) have been plotted within the field of the tholeiite series after Miyashiro (1974) and the remaining five samples belong to the calc-alkali rock series.

Next, the FeO*-FeO*/MgO diagram of the Fig. II-1-10 indicates that the samples T-3-R and T-7-R have been plotted within the field of the tholeiite series after Miyashiro and the remaining six samples belong to the calc-alkali rock series.

At last, the TiO_2-FeO*/MgO diagram of the Fig. II-1-11 indicates that three basalts have been plotted within the field of MORB (Mid-ocean ridge basalt)

after Shimazu et al. (1974) and two diorite porphyrites and dacite belong to IAT (Island arc tholeiite), although the samples T-3-R and T-7-R have been plotted out of the diagram due to high FeO*/MgO value of 11.30 and 6.60 respectively. The petrological study by the use of the above several diagrams has revealed that three basalts (M-1-R, PP-1-R, PP-2-R) in the ophiolite complex have been plotted within the field of MORB, but has not been able to reveal which of basalt or tholeiite or calc-alkali rock series three basalts belong to.

The petrological study also reveals that two diorite porphyrites (S-1-R, Ta-2-R) in the Merungin area have been plotted within the field of IAT (Island arc tholeiite) and belong to the calc-alkali rock series and that acidic to intermediate volcanic and pyroclastic rocks (T-1-R, T-3-R, T-7-R) have been roughly plotted in the field of IAT and the sample T-1-R (dacite) belongs to the calc-alkali rock series, while the samples T-3-R (rhyolite) and T-7-R (trachytic tuff) belong to the high alkali tholeiite series.

Table II-1-5 Assay Result of Rock Samples in Kinabalu Region

Locality	Sample Number	Rock Name	SiO_2 %	TiO_2 %	Al_2O_2 %	Fe_2O_3 %	FeO %	MnO %	MgO %	CaO %	Na_2O %	K_2O %	P_2O_5 %	Ig-loss %	Total	Au ppb	Ag ppm	Co ppm	Cr ppm	Cu ppm	Mo ppm	Ni ppm	Pb ppm	S %	Zn ppm
B-1	B-1-R	Orthopyroxenite	41.73	0.14	3.02	5.60	3.14	0.13	36.05	3.68	0.02	<0.01	0.04	6.09	99.65	7	0.6	86	1716	13	<1	1634	101	0.234	106
Km-1	Km-1-R	Granodiorite Porphyry	66.03	0.48	15.64	0.94	3.20	0.06	1.98	4.25	2.88	2.73	0.17	1.10	99.46	<1	<0.5	11	135	21	<1	19	21	0.067	61
K-1	K-1-R	Quartz Diorite Porphyry	61.72	0.67	14.79	2.93	3.20	0.14	3.02	4.10	2.47	4.10	0.28	2.20	99.62	<1	<0.5	17	123	20	<1	18	28	0.046	76
Lu-1	Lu-1-R	Quartz Monzonite Porphyry	59.23	0.70	14.19	0.99	5.47	0.11	3.91	5.10	2.41	3.96	0.28	3.20	99.55	<1	<0.5	21	126	44	<1	19	16	0.049	52
Lu-3	Lu-3-R	Quartz Monzonite Porphyry	60.05	0.71	14.67	1.53	4.97	0.12	3.79	5.11	2.46	3.83	0.28	2.27	99.79	<1	<0.5	21	142	38	<1	18	24	0.086	63
Lu-4	Lu-4-R	Quartz Monzonite Porphyry	61.52	0.63	14.22	0.84	4.66	0.12	2.80	4.22	1.77	4.25	0.27	3.92	99.22	<1	<0.5	15	120	16	<1	12	30	0.127	59
M-1	M-1-R	Basalt	47.22	1.26	14.70	2.76	6.16	0.16	6.33	11.07	3.05	1.18	0.14	5.27	99.30	<1	<0.5	42	209	24	<1	102	7	0.072	66
M-2	M-2-R	Serpentinite	39.86	0.09	1.53	6.91	1.13	0.09	35.92	0.68	0.15	0.06	0.03	13.22	99.67	3	<0.5	78	1143	15	<1	1577	1	0.024	41
Mo-1	Mo-1-R	Gabbro	52.02	1.16	15.32	2.03	7.54	0.16	5.07	4.63	5.49	0.13	0.10	5.69	99.34	<1	<0.5	35	49	11	<1	26	8	0.067	65
PP-1	PP-1-R	Basalt	48.00	0.54	12.71	2.53	6.16	0.22	12.15	9.49	2.68	0.04	0.06	4.81	99.39	<1	<0.5	52	454	61	<1	352	5	0.579	111
PP-2	PP-2-R	Basalt	50.31	0.76	15.11	2.07	6.54	0.16	8.26	9.05	4.34	0.03	0.08	2.68	99.39	<1	<0.5	39	306	86	<1	106	8	0.173	58
P-1	P-1-R	Harzburgite	40.73	0.15	3.50	3.65	3.83	0.13	35.89	3.12	0.10	<0.01	0.03	8.37	99.51	5	<0.5	84	1715	25	<1	1520	2	0.042	50
S-1	S-1-R	Diorite Porphyrite	61.39	0.58	16.74	2.99	2.70	0.09	2.23	4.89	2.92	3.09	0.25	1.74	99.61	<1	<0.5	15	84	23	<1	24	14	0.039	50
Ta-2	Ta-2-R	Diorite Porphyrite	64.33	0.53	15.55	1.46	3.46	0.10	2.19	5.07	2.59	2.82	0.23	1.46	89.79	<1	<0.5	13	150	26	<1	18	26	0.118	62
T-1	T-1-R	Strongly Altered Dacite	69.96	0.66	15.02	1.59	0.37	<0.01	0.75	0.09	0.04	3.67	0.16	7.11	99.43	7	<0.5	12	150	82	<1	16	166	1.197	61
T-3	T-3-R	Altered Rhyolite	65.50	0.65	19.35	0.97	0.26	<0.01	0.10	0.18	0.98	5.16	0.13	6.29	99.58	<1	<0.5	8	93	13	<1	7	36	0.375	20
T-4	T-4-R	Sandstone	84.28	0.41	8.95	0.79	0.31	<0.01	0.39	0.02	0.03	1.89	0.05	2.49	99.62	2	<0.5	<1	224	6	<1	7	12	0.023	5
T-7	T-7-R	Strongly Silicified Trachytic Tuff	64.25	0.64	15.61	5.30	0.31	0.01	0.77	0.15	0.09	7.19	0.18	5.01	99.51	28	1	23	173	98	<1	26	75	3.807	31

Figure II-1-7 $Na_2O + K_2O$ - SiO_2 Diagram of Volcanic to Hypabyssal Rock in Kinabalu Region

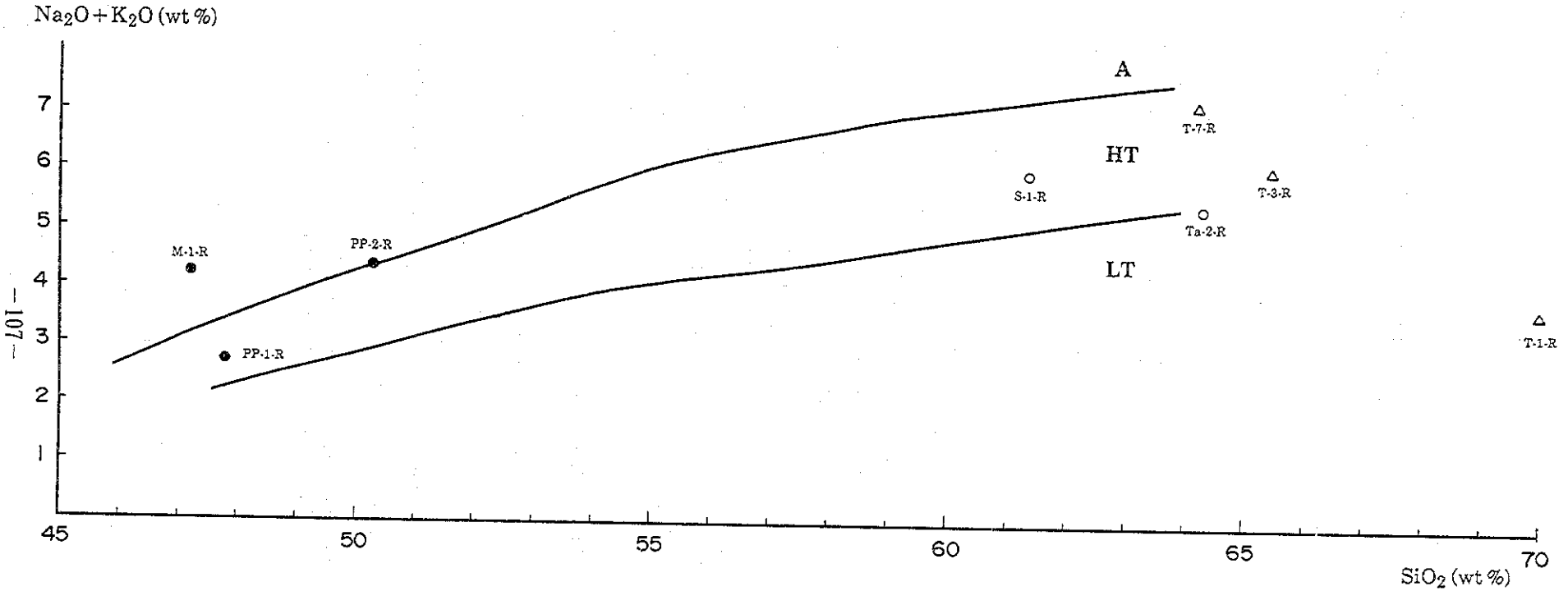

● : Basalt of ophiolite complex; ○ : Diorite porphyrite in Merungin area

△ : Volcanic and pyroclastic rock in Bt. Tampang area

A: Alkali basalt series; HT: High alkali tholeiite series, LT: Low alkali tholeiite series (after Kuno 1968)

Figure II-1-8 $FeO + Fe_2O_3$ - $Na_2O + K_2O$ - MgO Trigonal Diagram (MFA Diagram) of Volcanic to Hypabyssal Rock in Kinabalu Region

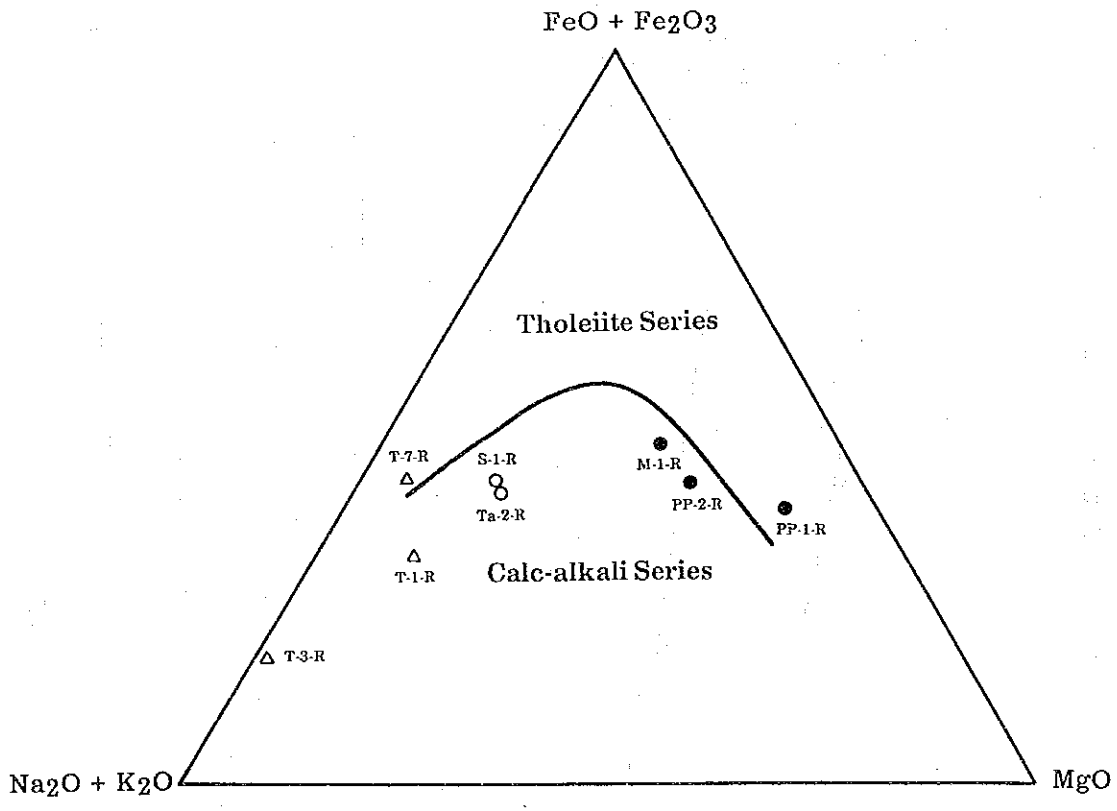

● : Basalt of ophiolite complex

o : Diorite porphyrite in Merungin area

△ : Volcanic and pyroclastic rock in Bt. Kampang area

Solid line is boundary between tholeiite series and calc-alkali series after Irvine and Barager (1971)

Figure II-1-9 SiO_2 - FeO*/MgO Diagram of Volcanic to Hypabyssal Rock in Kinabalu Region

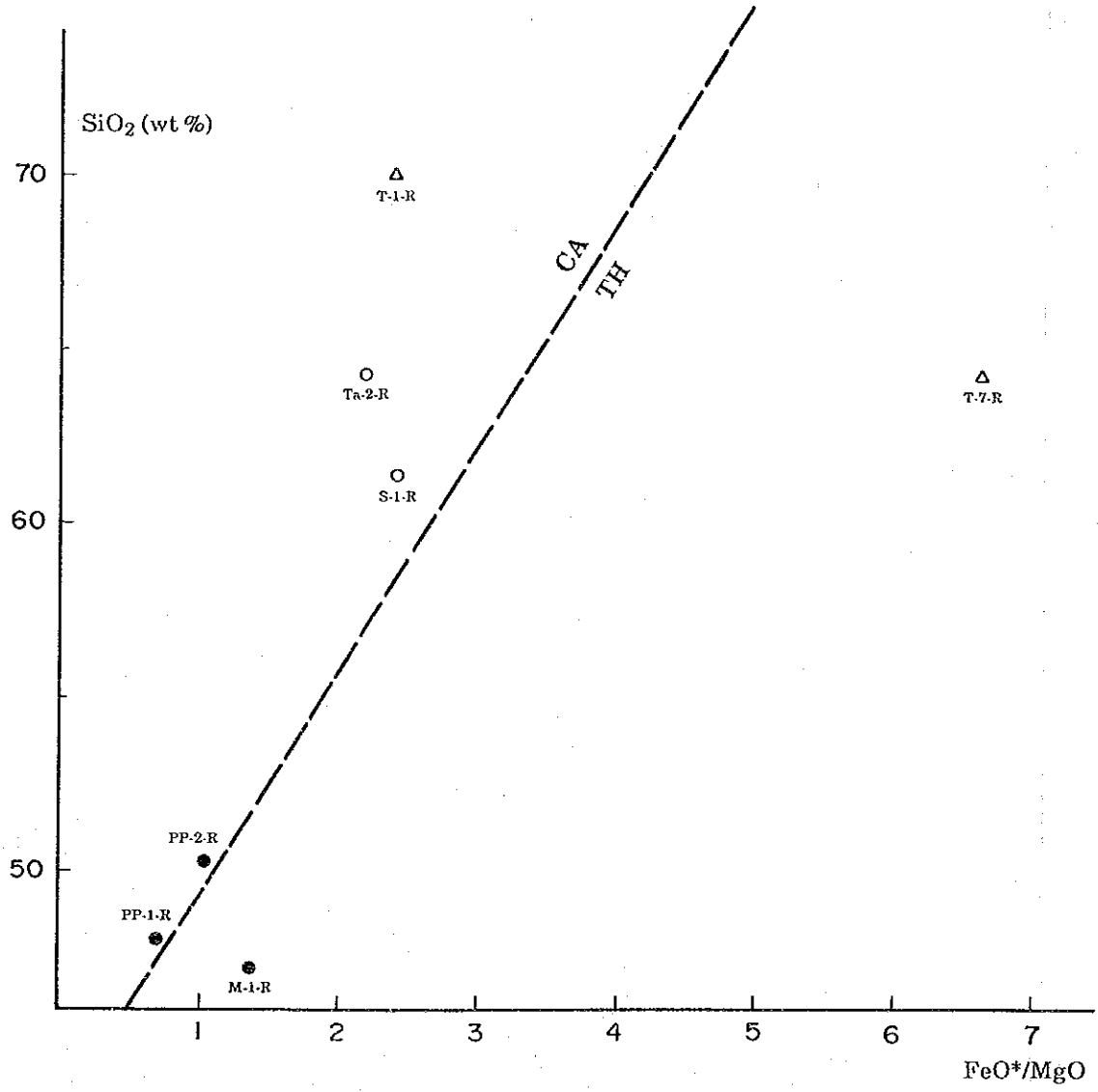

FeO*: Total Fe as FeO

● : Basalt of ophiolite complex　　o : Diorite porphyrite in Merungin area

△ : Volcanic and pyroclastic rocks in Bt. Kampang area

TH (tholeiitic) / CA (calc-alkaline) boundary: after Miyashiro, 1974

Figure II-1-10 FeO* - FeO*/MgO Diagram of Volcanic to Hypabyssal Rock in Kinabalu Region

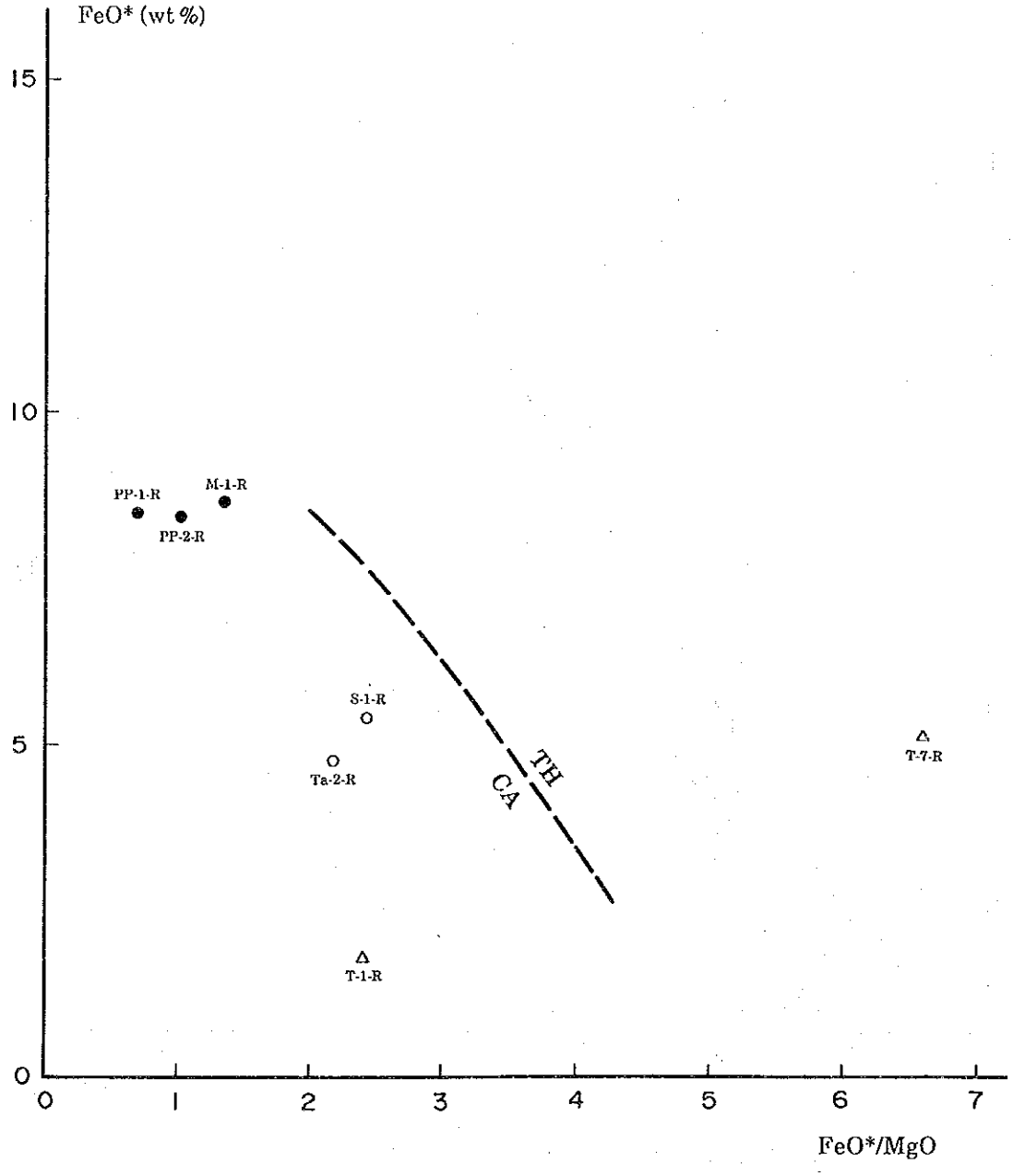

FeO*: Total Fe as FeO

● : Basalt of ophiolite complex, o : Diorite porphyrite in Merungin area

△ : Volcanic and pyroclastic rock in Bt. Tampang area

TH (tholeiitic) / CA (calc-alkaline) boundary: after Miyashiro, 1974

Figure II-1-11 TiO_2 - FeO*/MgO Diagram of Volcanic to Hypabyssal Rock in Kinabalu Region

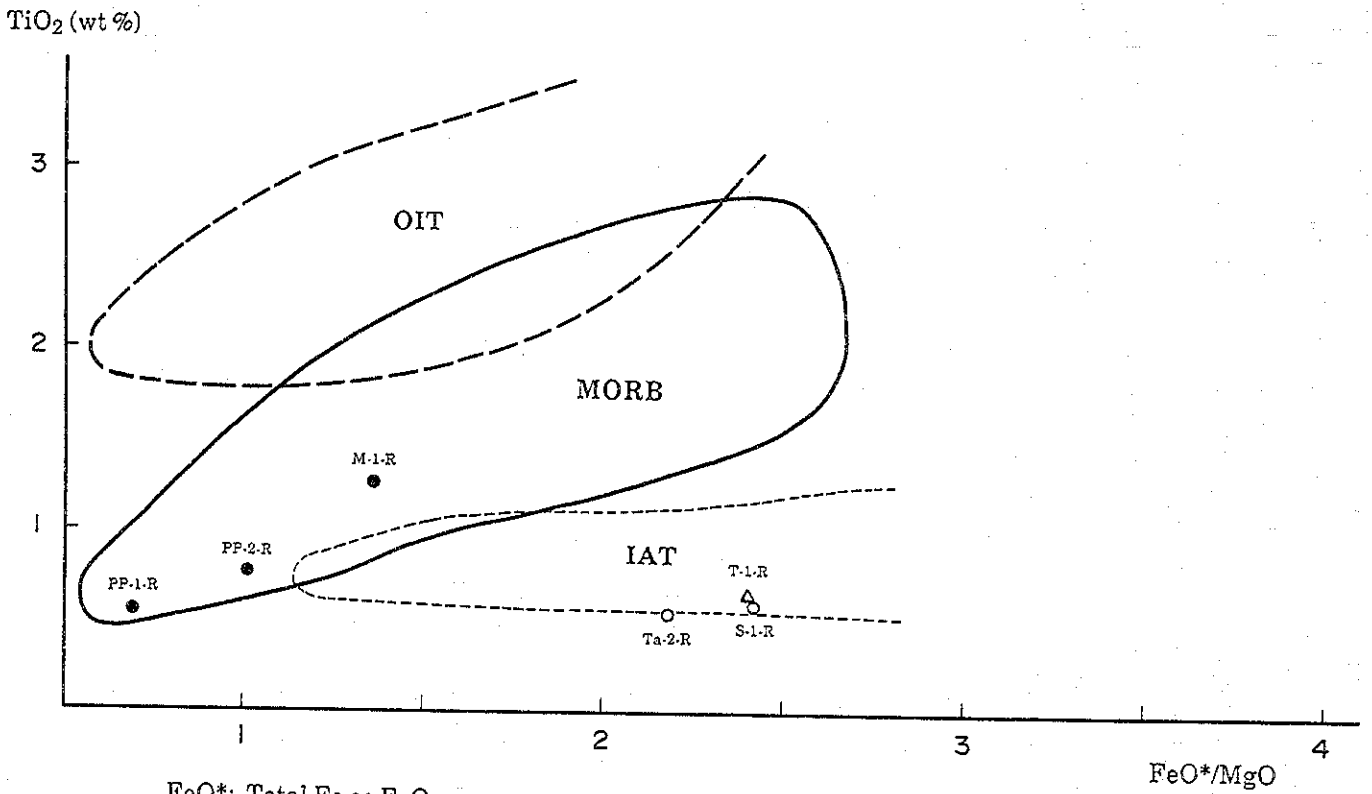

FeO*: Total Fe as FeO

● : Basalt of ophiolite complex, ○ : Diorite porphyrite in Merungin area

△ : Volcanic and pyroclastic rock in Bt. Tampang area

MORB: Mid-ocean ridge basalt; OIT: Oceanic island tholeiite
IAT : Island arc tholeiite (after Shimazu et al., 1990)

(3) Microscopic observation of thin section of rock (18 samples)

The thin sections made from 18 rock samples obtained at the same localities as the samples for the chemical analysis, namely 5 samples of acidic intrusive rock, found between Bt. Kiapako and Bt. Kamunsu, 2 samples of intermediate intrusive rock in the Kg. Merungin area, 4 samples of acidic to intermediate volcanic and pyroclastic rocks and sedimentary rock at the foot of Bt. Tampang, 3 samples of basalt, 1 sample of gabbro, and 3 samples of ultrabasic rock of the ophiolite complex, were observed under a polarization-microscope, and the result of the observation is shown in the Table II-1-6.

Table II-1-6 Result of Microscopic Observation of Thin Sections of Rock Samples taken in Kinabalu Region

Location	Sample Number	Rock Name	Texture	Phenocryst, Fragments									Groundmass, Matrix, Accessary Minerals										Alteration, Metamorphic Minerals											Remarks
				Quartz	Plagioclase	K-feldspar	Olivine	Augite	Hypersthene	Hornblende	Biotite	Others	Quartz	Plagioclase	K-feldspar	Augite	Hornblende	Biotite	Zircon	Apatite	Sphene	Opaque Minerals	Others	Quartz	Hornblende	Tremolite	Actinolite	Epidote	Zoisite	Biotite	Serpentine	Chlorite	Sericite	Calcite	Kaolinite	Others	
Kamunsu	Km-1-T	Granodiorite porphyry	porphyritic felsitic	○	◎	●				○	○		◎	◎			●	●	×	×		×	× *					×				×				
Kiapako	K-1-T	Quartz diorite porphyry	porphyritic hypidiomorphic granular		○	●		●		◎	○		○	◎	●		●	●	×	×		×										○	×				
Luminantai	Lu-1-T	Quartz monzonite porphyry	porphyritic hypidiomorphic granular		●	○		●		○	○		○	◎	○		●	●	×	×		●		●				×				◎	●	○			relatively strong alteration by chlorite and calcite
"	Lu-3-T	Quartz monzonite porphyry	porphyritic, felsic		●	○				◎	○		○	○	○				×		●	×										○	●	○			relatively strong alteration by chlorite and calcite, shows conspicuous myrmekite
"	Lu-4-T	Quartz monzonite porphyry	porphyritic hypidiomorphic granular		◎	●				* ◎	○		○	○	◎						●	** ●		●				●				○	◎	◎			* only pseudomorph remains, ** pyrite, strong alteration by calcite, serlcite, chlorite
Mankadau	M-1-T	Basalt	porphyritic intergranular		●			●						◎		◎					●		×										◎	◎			Slightly altered basalt with poor phenocryst
Pingan Pingan	PP-1-T	Basalt	porphyritic intergranular											◎		◎						●	* ◎								○	○		●			* picotite, phenocrysts (probably olivine, pyroxene, plagioclase) are totally altered
"	PP-2-T	Basalt	porphyritic subophitic		○			○						◎		◎					○	×		●				●				○					coarse basalt
Sasapan	S-1-T	Diorite porphyry	porphyritic, felsic		◎					○	○	* ×	●	◎				◎		●								×				×	×	●			* garnet
Tapap	Ta-2-T	Diorite porphyry	porphyritic, felsic		○					◎	●	* ×	●	◎				●		●		×								○			●				* garnet, secondary biotite surrounding hornblende phenocryst and in groundmass
Tampang	T-1-T	Dacite	porphyritic	○	○	○							◎	○					×			* ●			◎									○		* pyrite dissemination, strongly altered dacite
"	T-3-T	Rhyolite	porphyritic, felsic		○	○					●		◎	○	○				×			* ●			○							●	○		○		* pyrite dissemination, phenocrysts remain only as pseudomorphs, altered rhyolite
"	T-4-T	Sandstone	clastic	◎	●	●						* ●	◎																			●	○		●		* rock fragments of silt and chert, fine arkose sandstone
"	T-7-T	Trachytic tuff	pyroclastic	●		◎							◎		○				×			* ●			◎							●	◎		●		* pyrite, strongly silicified trachytic tuff

Location	Sample Number	Rock Name	Texture	Primary Minerals									Metamorphic, Alteration Minerals												Accessary Minerals									Remarks
				Plagioclase	Olivine	Augite	Hypersthene	Hornblende				Others	Hornblende	Cummingtonite	Actinolite	Tremolite	Epidote	Pumpellyite	Prehnite	Chlorite	Serpentine	Sericite	Calcite	Talc	Quartz	Others	Sphene	Picotite	Opaque					Others	
Bambangan	B-1-T	Orthopyroxenite	cataclastic			●	◎						◎							○	●		×						* ○						* Magnetite, cataclastic orthopyroxenite, hypersthene is replaced by cummingtonite.
Mankadau	M-2-T	Serpentinite	mesh																	○	◎			●				×	* ●						* Magnetite, orthopyroxene pseudomorph remains, originally hartzburgite.
Morouporou	Mo-1-T	Gabbro	hypidiomorphic granular	◎		○						* ○								○		●	○		●		○		●						* K-feldspar, relatively fine grain, altered gabbro.
Poring Road	P-1-T	Hartzburgite	cataclastic		◎	●	○														◎							●	●						Cataclastic hartzburgite

[Notes] ◎: Abundant, ○: Common, ●: Rare, ×: Trace

(4) Assay of ore sample (14 samples)

The assay result of 14 ore samples taken at 12 localities of mineral occurrence is shown in the Table II-1-9 in the following section 1-4.

(5) Microscopic observation of polished section of ore (7 samples)

The polished sections made from 7 samples of ore out of 14 ore samples taken for assay were observed under a ore microscope. The result of the observation is shown in the Table II-1-7. The Table II-1-7 shows that the boulder of Cyprus type massive cupriferous iron sulfide in the S. Lingangah (L-1-P) is high grade copper ore consisting of chalcopyrite, bornite, chalcocite, covellite, pyrite, and a very small amount of sphalerite and the float of high grade stibnite ore in the Kg. Randagong area (R-5-P) is mostly composed of stibnite with a trace of pyrite and that ore at the T-3 locality of mineral occurrence in hydrothermally altered rock at the foot of Bt. Tampang is disseminated ore consisting of minor amounts of chalcopyrite and pyrite and a trace of sphalerite.

Table II-1-7 Result of Microscopic Observation of Polished Sections of Ore Samples from Kinabalu Region

Locality Name	Lingangah	Pingan Pingan	Randagong	Randagong	Randagong	Tampang	Tampang
Sample Number	L-1-1	PP-2-P	R-1-P	R-2-P	R-5-P	T-1-P	T-3-P
Occurrence	High grade Cu ore	Pyrite veinlet and dissemination	Limonite (from oxidized outcrop?)	Limonite (from oxidized outcrop?)	Stibnite ore	Pyrite-quartz veinlet	Chalcopyrite-pyrite dissemination
Chalcopyrite	○	・					●
Bornite	○						
Chalcocite	○						
Covellite	○						
Sphalerite	・						・
Galena							
Pyrite	●	●			・	●	●
Magnetite							
Hematite			・	・			
Limonite (mostly geothite)			◎	◎			
Stibnite					◎		
Gangue minerals (Q: Quartz)	・	◎	○Q	○Q	○Q	◎Q	◎
Remarks					partly weathered with stibiconite		

[Notes] ◎: Abundant, ○: Common, ●: Rare, ・: Trace

(6) X-ray diffraction examination of hydrothermally altered rock (15 samples)

The result of the X-ray diffraction examination of 15 hydrothermally altered rock samples, namely 3 samples taken from hydrothermal alteration veins along parallel joints in quartz monzonite porphyry around Bt. Luminantai and 12 samples from hydrothermally altered acidic to intermediate volcanic and pyroclastic rocks and sedimentary rock around Bt. Tampang, for the identification of hydrothermal alteration minerals is shown in the Table II-1-8. The Table II-1-8 indicates that hydrothermal alteration veins around Bt. Luminantai consist of a large quantity of quartz, a middle quantity to a trace of potash felspar, a small quantiy to a trace of sericite, a trace of kaolinite, and a trace of chlorite and that hydrothermal alteration zone found at the foot of Bt. Tampang is composed mainly of a large quantity of quartz, a small quantity to a trace of kaolinite, a trace of chlorite, and a trace of sericite, and contains, in places, a middle to small amount of potash felspar (T-3-X, T-6-X), a trace of smectite (T-9-X, T-10-X), a trace of pyrite (T-3-X, T-7-X), a trace of hematite (T-5-X), and a trace of magnetite (T-2-X) in addition to the above four minerals.

The X-ray diffraction examination reveals that the mineral assemblage of the hydrothermal alteration veins in quartz monzonite porphyry around Bt. Luminantai and the hydrothermal alteration zone at the foot of Bt. Tampang is similar to that of the upper part of the hydrothermal alteration zone accompanying epithermal gold deposit of the adularia-sericite type (Hayba et al., 1986; Heald et al., 1987) or of low sulfidation system (Hedenquist, 1987) formed by intermediate to weak alkaline hydrothermal liquid, or is similar to that of the SCC zone (sericite, clay, chlorite) proposed by Sillitoe et al. (1984) accompanying the upper part of porphyry copper deposit in the Philippines.

Table II-1-8 Result of X-ray Diffraction of Hydrothermally Altered Rock in Kinabalu Region

Area	Sample Number	Clay Minerals					Others				
		Kaolinite	Pyrophyllite	Sericite	Smectite	Chlorite	Quartz	K-felspar	Pyrite	Hematite	Magnetite
Luminantai	Lu-2-X	×		●		×	◎				
"	Lu-3-X	×		×		×	◎	○			
"	Lu-5-X	×	×			×	◎	×			
Tampang	T-1-X	●		×		×	◎				
"	T-2-X	●		×		×	◎				×
"	T-3-X	●		×		×	◎	●	×		
"	T-4-X	×		×		×	◎				
"	T-5-X	×		×		×	◎			×	
"	T-6-X	●				×	◎				
"	T-7-X	×		×		×	◎	○	×		
"	T-8-X	×		×		×	◎				
"	T-9-X	×		×	×	×	◎				
"	T-10-X	×		×	×	×	◎				
"	T-11-X	×		×		×	◎				
"	T-12-X	×		×		×	◎				

[Notes] ◎: Abundant, ○: Common, ●: Rare, ×: Trace

(7) Measurement of homogenization temperature of fluid inclusions in quartz (10 samples)

Homogenization temperature of fluid inclusions in 10 quartz samples, namely 4 samples (T-1-Q-1, T-1-Q-2, T-3-Q, T-10-Q) taken from (gold)-pyrite-limonite-bearing quartz veinlets in the hydrothermal alteration zone at the foot of Bt. Tampang, 1 sample (Lu-3-Q) from limonite-bearing quartz veinlet accompanying hydrothermal aleration vein along joint in quartz monzonite porphyry around Bt. Luminantai, and 4 samples (R-1-Q, R-2-Q, R-3-Q, R-5-Q) from limonite-bearing quartz veins and 1 sample (R-4-Q) from quartz vein in the Trusmadi Formatin in the Kg. Randagong area, were measured to study the formation temperature of quartz.

The histgrams of the homogenization temperature measured are shown in the Fig. II-1-12, II-1-13 and II-1-14.

The Fig. II-1-12 shows that the homogenization temperatures of four samples from the Bt. Tampang area are 219° to 237°C (average 228°C), 218° to 256°C (average 237°C), 232° to 259°C (average 248°C), and 278° to 284°C (average 281°C) respectively, after excepting the temperature of only one inclusion at the higher and lower temperature parts.

The Fig. II-2-13 and II-2-14 indicate that the homogenization temperature of five samples of the Kg. Randagong area are 155° to 217°C (average 181°C), 171° to 181°C (average 178°C), 173° to 201°C (Average 185°C), 180° to 199°C (average 189°C), and 183° to 212°C (average 196°C) respectively and that the homogenization temperature of one sample of the Bt. Luminantai area ranges from 350° to 417°C and is considerably higher than those of other nine samples.

The measurement of the homogenization temperature reveals that the homogenization temperature of 4 samples of the Bt. Tampang area ranges from 218° to 284°C and is included in the range of 200° to 300°C of high sulfidation system epithermal gold deposit (Hedenquist, 1987) accompanying hydrothermal liquid related to the volcanic activety in the Circum-Pacific region, rather than the range of 170° to 270°C of that of the low sulfidation system, or is included in the range of 133° to 349°C of the adularia-sericite type or in the range of 120° to 320°C of the acid-sulfate type gold deposit in the western Pacific island arcs region. (Sillitoe, 1988)

Fig. II-2-13 and II-2-14 show that the homogenization temperature of limonite-bearing quartz veins in the Kg. Randagong area ranges from 155° to 217°C and is lower than that of (gold)-limonite-pyrite-bearing quartz veinlets around Bt.

Tampang.

The homogenization temperature of 350° to 417°C (average 384°C) of limonite-bearing quartz veinlet accompanying hydrothermal alteration vein in the Bt. Luminantai area is included in the range of that of quartz vein accompanying porphyry copper deposit (300° to 480°C in case of Mamut deposit; after Nagano et al., 1977). However, owing to a lack of the number of the sample, a definite conclusion about the above must be reserved.

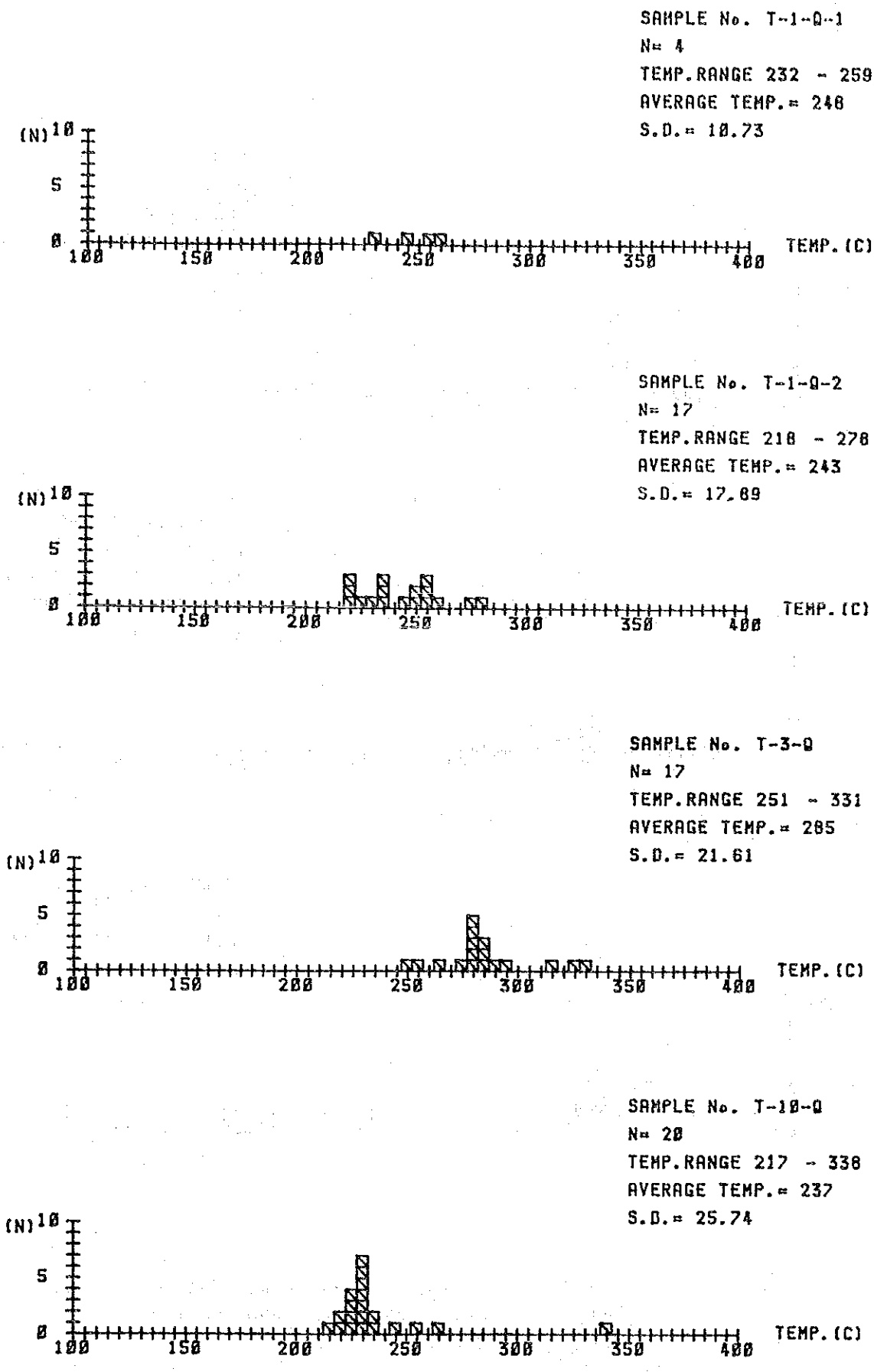

Figure II-1-12 Histgrams of Homogenization Temperature of Fluid Inclusions in Quartz from Bt. Tampang Area (T-1-Q-1, T-1-Q-2, T-3-Q, T-10-Q)

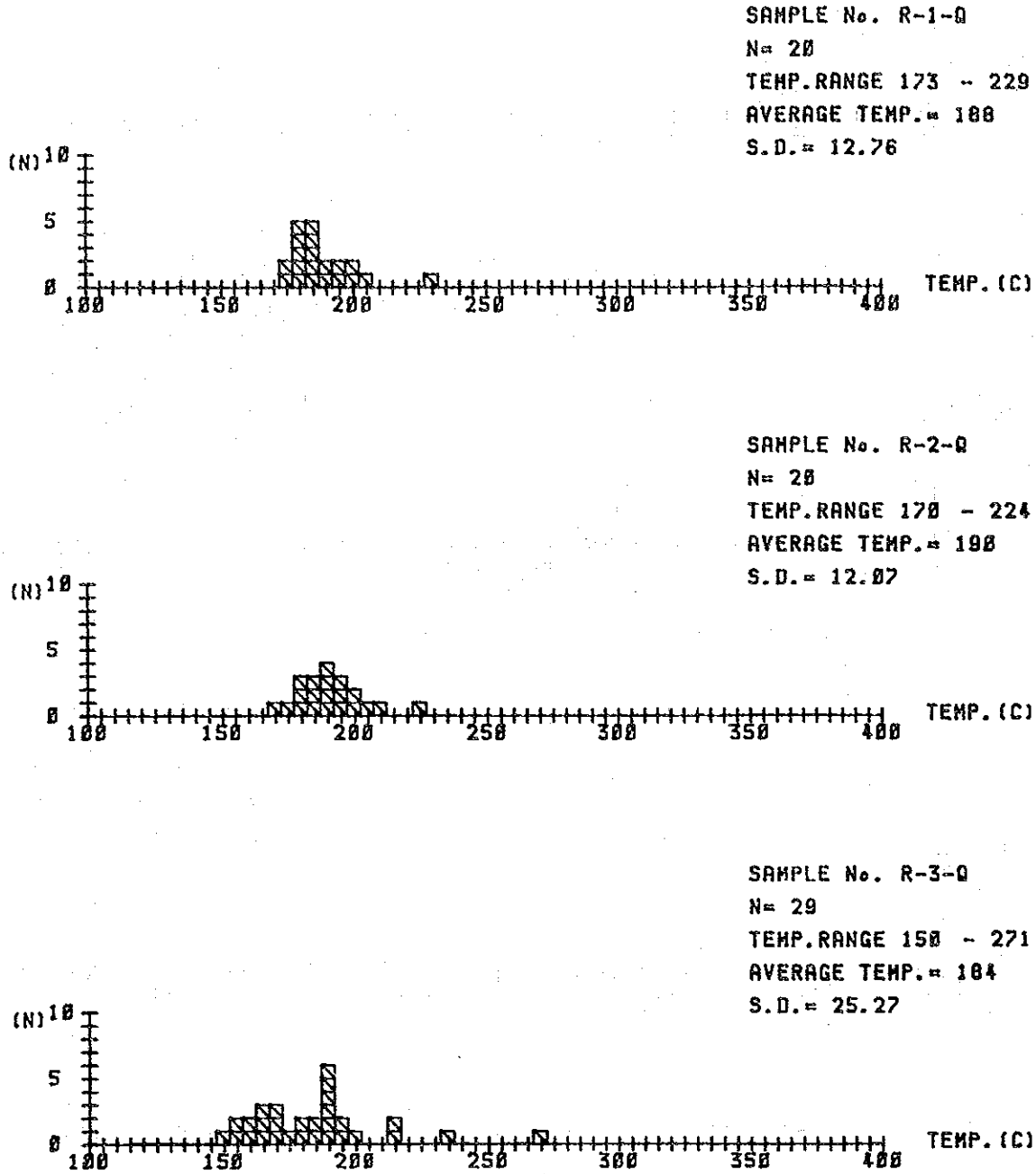

Figure II-1-13 Histgrams of Homogenization Temperature of Fluid Inclusions in Quartz from Kg. Randagong Area (R-1-Q, R-2-Q-R-3-Q)

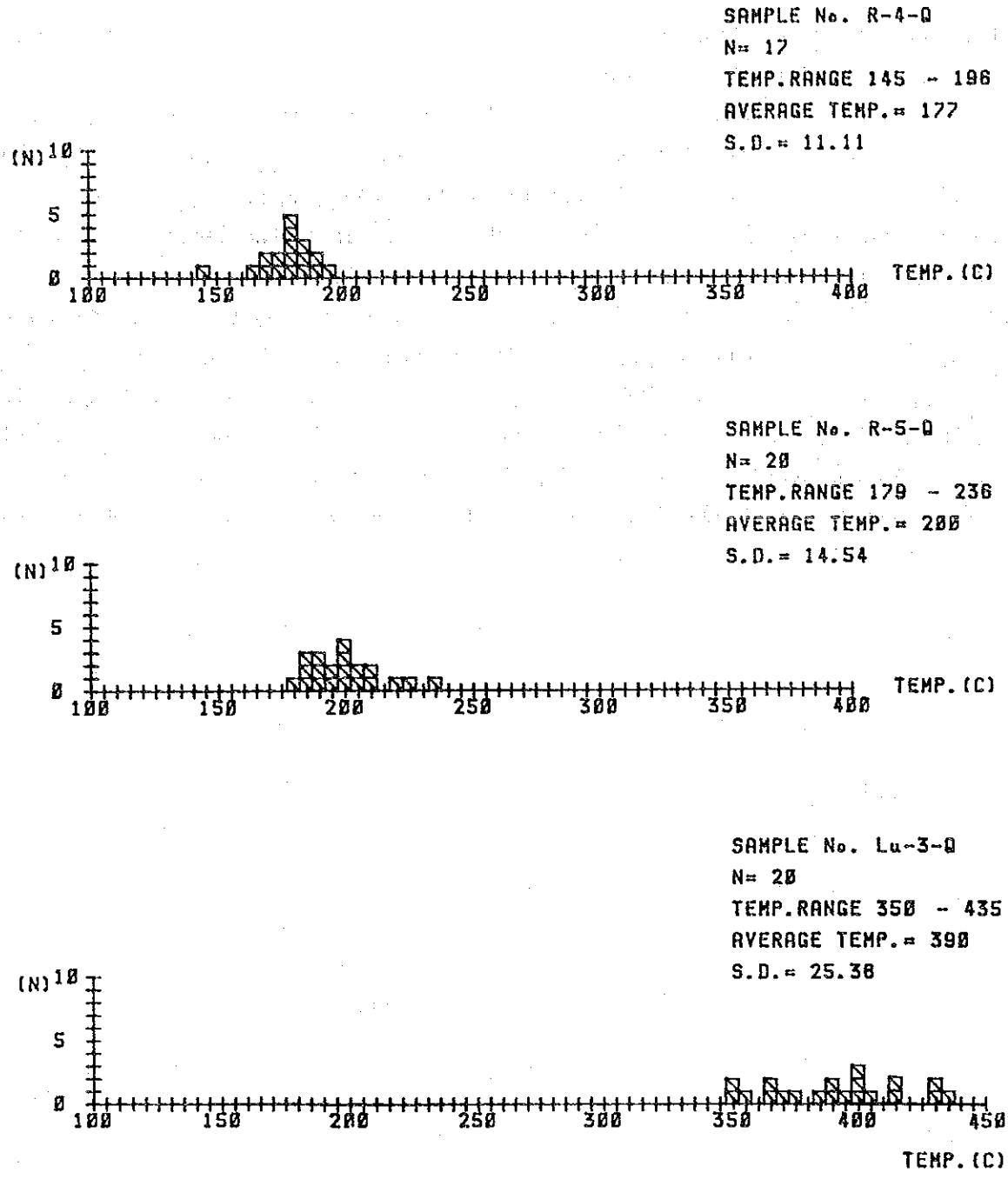

Figure II-1-14 Histgrams of Homogenization Temperature of Fluid Inclusions in Quartz from Kg. Randagong and Bt. Tampang Areas (R-4-Q, R-5-Q, Lu-3-Q)

1-4 Assay Result of Ore (14 samples)

The assay result of 14 ore samples taken at 12 localities of mineral occurrence investigated is shown in the Table II-1-9.

The assay result reveals that boulder of Cyprus type massive cupriferous iron sulfide in the S. Lingangah (sample L-1-0) contains 2.63 g/t Au, 216.8 g/t Ag, and 36.58% Cu and boulder of stibnite ore in the Kg. Randagong area (sample R-5-0-2) contains 23.79% Sb, as anticipated from the megascopical observation of the both samples taken at the investigation of the localities of mineral occurrence.

The assay result also reveals that limonite network embedded in guartz monzonite porphyry forming Bt. Luminantai (sample Lu-2-0) contains 2.45% Pb, 0.10% Cu, 0.13% Zn, and 11.1 g/t Ag and that 2.68 g/t of Au is contained in limonite-bearing quartz veinlet (sample T-10-0) embedded in hydrothermally altered rock found at the foot of Bt. Tampang and pyrite-limonite-bearing quartz veinlets in the same hydrothermally altered rock contain 0.13% Sb (T-1-0-1), 0.16% Pb and 22.05 ppm Hg (T-1-0-2), and 22.45 ppm Hg (T-3-0) respectively.

Table II-1-9 List of Assay Result of Ore Samples taken in Kinabalu Region

Locating	Sample Number	Au g/t	Ag g/t	Cu ppm	Fe %	Hg ppb	Mo ppm	Pb ppm	S %	Sb ppm	Zn ppm	Occurrence of Ore
L-1	L-1-0	2.63	216.8	365,800	18.41	74	342	581	32.92	12	602	boulder of Cyprus type massive sulfide
Lu-2	Lu-2-0	0.10	11.1	1,015	28.92	124	<1	24,550	0.30	46	1,304	stockwork of limonite
Lu-3	Lu-3-0	<0.01	<0.1	51	4.67	<10	<1	88	0.01	6	178	stockwork of limonite·quartz
PP-2	PP-2-0	<0.01	<0.1	448	5.13	319	<1	12	2.33	6	6,159	Cyprus type limonitte·pyrite·quartz·malachite stockwork
R-1	R-1-0	<0.01	<0.1	28	34.96	122	<1	12	0.01	2	636	quartz·limonite vein
R-2	R-2-0	<0.01	<0.1	25	15.27	1,002	<1	26	0.06	2	300	quartz·limonite vein
R-3	R-3-0	<0.01	<0.1	33	5.04	1,427	2	22	0.09	25	30	quartz·limonite vein
R-5	R-5-0-1	<0.01	<0.1	22	6.05	1,162	<1	15	0.62	27	86	quartz·limonite·pyrite·stibnite vein
R-5	R-5-0-2	<0.01	<0.1	48	1.40	9,300	<1	127	9.72	237,900	41	boulder of stibnite-pyrite ore
T-1	T-1-0-1	<0.01	<0.1	20	3.43	2,470	6	207	3.68	1,267	89	stockwork of quartz·pyrite·limonite veinlets
T-1	T-1-0-2	<0.01	<0.1	20	1.31	22,050	2	1,581	0.20	101	31	stockwork of quartz·pyrite·limonite veinlets
T-3	T-3-0	<0.01	<0.1	29	2.15	22,450	1	128	1.94	36	25	lens of pyrite · limonite · quartz
T-7	T-7-0	<0.01	1.3	76	2.52	2,825	2	85	2.50	25	34	lens of pyrite · limonite
T-10	T-10-0	2.68	0.1	91	13.98	5,575	<1	107	0.04	149	23	quartz·limonite veinlets

1-5 Consideration

The conclusion obtained from the results of the investigation of the localities of mineral occurrence and the laboratory works on the samples of rock, ore, quartz, and so on is summarized below.

(1) The mineralized zone of veinlets, 1 ~ 10 cm wide, network, and dissemination, consisting of quartz with minor amounts of pyrite and limonite, embedded in acidic to intermediate volcanic and pyroclastic rocks subjected to hydrothermal alteration, is found at the western and southern foots of Bt. Tampang.
This gold-bearing mineralized zone seems to correspond to the upper part of epithermal gold deposit accompanying intermediate to weak alkaline hydrothermal fluid related to the volcanic activity which probably took place during Miocene to Pliocene time, judging from the fact that some veinlets in the mineralized zone contain gold (2.68 g/t), antimony (0.13%), and mercury (22.05 ppm, 22.45 ppm) and the hydrothermal alteration mineral assemblage of hydrothermally altered rock consists mainly of quartz, sericite, kaolinite, and chlorite, accompanied, in places, by some potash felspar and smectite and that homogenization temperature of the fluid inclusion in quartz taken from quartz veinlets ranges from 218° to 259°C except for 278° to 284°C of one sample.

(2) The veined hydrothermal alteration zones accompanied partly by some limonite and quartz are found along many parallel joints in quartz monzonite porphyry around Bt. Luminantai. Hydrothermal alteration veins are narrow in width (1 to 30 cm) and form network as a whole.
There is a possibility possible that these hydrothermal alteration veins may correspond to the SCC zone (sericite-clay-chlorite) accompanying the upper part of porphyry copper deposit, considering that some limonite·quartz veinlet in hydrothermal alteration vein contains Pb (2.46%), Zn (0.13%), Cu (0.10%), and Ag (11.1 g/t) and the mineral assemblage of hydrothermal alteration vein consisting mainly of quartz, chlorite, kaolinite, potash felspar, and sericite is similar to that of the SCC zone, proposed by Sillitoe et al. (1984), accompanying the upper part of porphyry copper deposit in the Philippines, and that the homogenization temperature of fluid inclusion in quartz taken from limonite·quartz veinlet in hydrothermal alteration vein ranges from 350° to 417°C and is included in the range of that of quartz vein accompanying porphyry copper deposit (300° to 480°C in case of Mamut deposit, after Nagano et al., 1977).

However, seeing that ore samples for chemical analysis (2 samples), clay samples for X-ray diffraction (3 samples), and quartz sample for measurement of homogenization temperature (1 sample) are short of the number and that quartz monzonite porphyry between hydrothermal alteration veins has not been subjected to hydrothermal alteration, a definite conclusion about the above must be reserved.

(3) The ages of acidic to intermediate intrusive rocks, which are roughly aligned in the direction of the north-south from Kg. Tagap to Bt. Kamunsu including quartz monzonite porphyry around Bt. Luminantai, have been determined as 6.85±0.17 to 7.47±0.20 Ma (late Miocene) by the K-Ar method of whole rock and are 1.5 to 2.1 Ma younger than 9.0 Ma of Kinabalu batholith.

(4) The mineralized zone of Cyprus-type networked and disseminated cupriferous iron sulfide, consisting of pyrite with a trace of sphalerite and malachite, in pillow basalt of the ophiolite complex is found in the old adit about two kilometers east of Kg. Pingan Pingan situated along Marudu Bay in northern Sabah.

Considering that the mineralized zone contains 0.62% of zinc and no copoper and is small in extent, it seems that mineralization here might be weak.

(5) Four outcrops of limonite-bearing quartz veins embedded in faults in the alternating beds of sandstone and shale (sandstone ≫ shale) of Trusmadi Formation and floats of high grade stibnite are found in the Samalang river basin in the Randagong area.

The assay result reveals that no useful metal including antimony is contained in the samples taken at four outcrops of limonite-bearing quartz veins. Therefore, it seems that limonite in limonite-bearing quartz vein has probably been formed by oxidation of pyrite and floats of high grade stibnite have been possibly derived from the partial concentration of stibnite in pyrite·quartz vein.

(6) The chemical analyses of the representative rock samples have been plotted on several diagrams for the petrological study.

The result obtained from the TiO_2-FeO*/MgO diagram reveals that three basalts of the ophiolite complex have been plotted within the field of MORB (Mid-ocean ridge basalt) and two diorite porphyrites of the Kg. Merungin area and three samples of acidic to intermediate volcanic and pyroclastic rocks in the Bt. Tampang area belong roughly to IAT (Island arc tholeiite) series. (FeO*:

calculated as total FeO from the analyses of FeO and Fe_2O_3)

CHAPTER 2 LABUK REGION

2-1 Contents of the Survey

2-1-1 Investigation of Locality of Mineral Occurrence

In order to understand geology and mineralization at the localities of mineral occurrence in the Labuk Region and then clarify the characteristic of mineralization in the region, 28 localities of mineral occurrence of Cyprus type massive, networked, and disseminated iron sulfide embedded in basalt and dolerite of the ophiolite complex, namely 13 localities in the Bidu Bidu Hills area; 1 in East Sualog, 2 in Kiabau, 3 in Porog, 3 in Southwest Sualog, 1 in Ulu West Sualog, 3 in West Sualog; and 15 localities in the Telupid area; 1 (Tg-1) at the riverside of the S. Unsadan, a tributary of the S. Tungud, 1 (E-1) at the roadside in the upper reaches of the S. Ensuan, 1 (TE-1) at the Forestry Training Institute site in Telupid, 11 (ST-2 ~ ST-6, ST-9 ~ ST-13, ST-15) along the S. Telupid to the southwest of Telupid, 1 (Kg-2) at the riverside of the S. Karang, a tributary of the S. Karamuak, were investigated. The locations of mineral occurrences investigated are shown in the Fig. II-2-1 attached at the end of this report.

2-1-2 Laboratory work

The following laboratory works on the samples of ore and host rock obtained at the localities of mineral occurrence and on the representative rock samples taken near the localities of mineral occurrence were conducted for the purpose of understanding mineralization at the localities of mineral occurrence and geology at and around the localities of mineral occurrence in the Labuk region.
The list of the samples taken is shown in the Table II-2-1 and locations of the samples are shown in the Fig. II-2-2 attached at the end of this report.

(1) K-Ar age determination of rock (11 samples)

Eleven representative rock samples taken from the ophiolite complex, namely 4 samples of basalt, 5 samples of dolerite, and 2 samples of gabbro, out of 32 rock samples taken for microscopic observation and chemical analysis, were dated by the K-Ar method of whole rock.

(2) Chemical analysis of rock sample (32 samples)

Thirty-two rock samples in total, namely 11 samples taken at the same localities as the samples for the K-Ar age determination, 7 samples of basalt, 3 samples of dolerite, 2 samples of gabbro, and 9 samples from ultrabasic rock in the ophiolite complex, were chemically analyzed.

(3) Microscopic observation of thin section of rock (32 samples)

The thin sections were made from 32 rock samples obtained at the same localities as the samples for chemical analysis and were observed under a polarization-microscope.

(4) Assay of ore (46 samples)

Forty-six samples taken in the Bidu-Bidu Hills and Telupid areas, namely 34 ore samples taken from 28 localities of mineral occurrence of Cyprus type cupriferous iron sulfide and 12 samples of Cr-Ni-bearing laterite formed by the weathering of ultrabasic rock were assayed.

(5) Microscopic observation of polished section of ore (23 samples)

Twenty-three polished sections were made from ore samples taken at 23 localities out of 34 ore samples obtained at 28 localities of mineral occurrence investigated and then were observed under a ore microscope.

Table II-2-1 List of Samples taken in Labuk Region for Laboratory Work

Locality Name	Locality Number	Dating	Analysis of Rock	Thin Section	Assay of Ore	Polished Section	X-ray Defraction	Fluid Inclusion	Specimen
Boto	Bo-1				Bo-1-0-L				
Chromite	Cr-1		Cr-1-R	Cr-1-T					
East Sualog	ES-1	ES-1-D	ES-1-R	ES-1-T					ES-1-D-S
"	ES-2		ES-2-R	ES-2-T					
"	ES-3		ES-3-R	ES-3-T	ES-3-0	ES-3-P			ES-3-0-S
Ensuan	E-1	E-1-D	E-1-R	E-1-T	E-1-0	E-1-P			E-1-D-S
"	"								E-1-0-S
Gambaran	Ga-1		Ga-1-R	Ga-1-T	Ga-1-0-L				
"	Ga-2				Ga-2-0-L				
Karamuak	Kr-1		Kr-1-R	Kr-1-T	Kr-1-0-L				
Karang	Kg-1	Kg-1-D	Kg-1-R	Kg-1-T					Kg-1-D-S
"	Kg-2				Kg-2-0	Kg-2-P			
Kiabau	KB-1				KB-1-0	KB-1-P			KB-1-0-S
"	KB-2	KB-2-D	KB-2-R	KB-2-T					KB-2-D-S
"	KB-3		KB-3-R	KB-3-T	KB-3-0				
Northeast Sualog	NE-1				NE-1-0-L				
Porog	Po-1				Po-1-0	Po-1-P			
"	Po-2		Po-2-R	Po-2-T	Po-2-0	Po-2-P			Po-2-0-S
"	Po-3				Po-3-0	Po-3-P			Po-3-0-S
Pumadagan	Pm-1		Pm-1-R	Pm-1-T	Pm-1-0-L				
Ruku Ruku	Rk-1				Rk-1-0-L				
Southwest Sualog	SW-1		SW-1-R	SW-1-T	SW-1-0	SW-1-P			SW-1-0-S
"	SW-2	SW-2-D	SW-2-R	SW-2-T					SW-2-D-S
"	SW-3		SW-3-R	SW-3-T					
"	SW-4		SW-4-R	SW-4-T					
"	SW-5		SW-5-R	SW-5-T	SW-5-0	SW-5-P			SW-5-0-S
"	SW-6		SW-6-R	SW-6-T	SW-6-0-1				
"	"				SW-6-0-2	SW-6-P			SW-6-0-2-S
"	SW-7		SW-7-R	SW-7-T	SW-7-0-L				
Sualog/Pari	SP-1	SP-1-D	SP-1-R	SP-1-T					
Sungai Telupid	ST-1	ST-1-D	ST-1-R	ST-1-T					ST-1-D-S
"	ST-2				ST-2-0				

Locality Name	Locality Number	Dating	Analysis of Rock	Thin Section	Assay of Ore	Polished Section	X-ray Defraction	Fluid Inclusion	Specimen
Sungai Telupid	ST-3				ST-3-0-1	ST-3-P			ST-3-0-1-S
"	"				ST-3-0-2				
"	ST-4				ST-4-0				
"	ST-5				ST-5-0				
"	ST-6				ST-6-0	ST-6-P			
"	ST-7		ST-7-R	ST-7-T					
"	ST-8		ST-8-R	ST-8-T					
"	ST-9		ST-9-R	ST-9-T	ST-9-0	ST-9-P			
"	ST-10				ST-10-0				
"	ST-11				ST-11-0-1				
"	"				ST-11-0-2	ST-11-P			
"	ST-12				ST-12-0-1	ST-12-P			ST-12-0-1-S
"	"				ST-12-0-2				
"	ST-13				ST-13-0	ST-13-P			ST-13-0-S
"	ST-14		ST-14-R	ST-14-T					
"	ST-15				ST-15-0	ST-15-P			ST-15-0-S
Tangkunap	TP-1				TP-1-0-L				
Telupid	TE-1	TE-1-D	TE-1-R	TE-1-T	TE-1-0	TE-1-P			TE-1-0-S
"	TE-2				TE-2-0-L				
"	TE-3				TE-3-0-L				
Tungud	Tg-1	Tg-1-D	Tg-1-R	Tg-1-T	Tg-1-0-1	Tg-1-P			Tg-1-D-S
"	"				Tg-1-0-2				Tg-1-0-1-S
Ulu Pari	UP-1		UP-1-R	UP-1-T	UP-1-0-L				
Ulu West Sualog	UWS-1	UWS-1-D	UWS-1-R	UWS-1-T					UWS-1-D-S
"	UWS-2		UWS-2-R	UWS-2-T	UWS-2-0	UWS-2-P			UWS-2-0-S
West Sualog	WS-1				WS-1-0	WS-1-P			WS-1-0-S
"	WS-2	WS-2-D	WS-2-R	WS-2-T					WS-2-D-S
"	WS-3		WS-3-R	WS-3-T	WS-3-0	WS-3-P			
"	WS-4				WS-4-0				
"	WS-5				WS-5-0	WS-5-P			WS-5-0-S
Total		11	32	32	46(34+12)	23			26

2-2 Geology

The geology of the Labuk region is represented by that of the Bidu-Bidu Hills area, and the stratigraphy of the Bidu-Bidu Hills area is summarised in Table II-2-2. The oldest rocks exposed are schists and coarse-grained quartzo-feldspathic rocks belonging to the Crystalline Basement of pre-Upper Cretaceous age. The overlying Chert-Spilite formation of Upper Cretaceous to Palaeocene age comprises an eugeosynclinal suite of spilite, volcanic breccia, mudstone, sandstone, ultrabasic conglomerate, and chert. Ultrabasic plutonic rocks were probably intruded during the deposition of the Chert-Spilite Formation. Eugeosynclinal flysch-type deposition continued in Eocene and early Oligocene times with the accumulation of the Crocker Formation comprising alternations of grey sandstone and grey, greyish-red, and purple shale. Shallower water conditions prevailed during the late Oligocene and early Miocene with the deposition of the Kulapis Formation and the Kamansi and Tambang Beds. The Kulapis Formation comprises chocolate-coloured calcareous sandstone and chocolate-coloured shale and mudstone. The Kamansi Beds consist of medium- to coarse-grained sandstone, shale, and thin carbonaceous laminae, and the Tambang Beds comprise fine- to medium-grained, commonly calcareous sandstone and grey shale.

Following the deposition of the Tambang Beds folding in mid-Miocene time caused intense deformation and uplift of the pre-Upper Miocene sedimentary rocks and was accompanied by the intrusion of basic igneous rock. During or following the folding widespread slump deposits accumulated, represented in the Bidu-Bidu Hills area by the Garinono Formation which comprises sub-rounded blocks of varying size and lithology in a matrix of grey clay. The succeeding Bongaya Formation is a shallow-water, deltaic sequence of white sandstone and grey carbonaceous shale with thin coaly laminae. Recent alluvium has accumulated over large areas of the Labuk Delta and also along the larger river valleys. Colluvial material flanks many of the mountains, and merges with the alluvium in the valley bottoms.
(taken from Newton-Smith, J., 1967)

Table II-2-2 Stratigraphy of the Bidu-Bidu Hills Area

AGE	TERTIARY LETTER CLASSIFICATION	SEDIMENTARY ROCKS	IGNEOUS ROCKS	ABSOLUTE AGE m.y.	PALAEOGEOGRAPHY AND DIASTROPHISM
HOLOCENE		RECENT ALLUVIUM : boulder gravel			Erosion
PLEISTOCENE	Th	PINOSUK GRAVELS clayey to sandy boulder gravel	Uplift of Kinabalu pluton	15	Glacial and periglacial erosion and re-deposition Uplift and differential warping
PLIOCENE	Tg	Non-deposition			Peneplanation
MIOCENE	Tf		Intrusion of the Kinabalu batholith : mainly adamellite	7 9	
		(WARIU FORMATION : slump breccia)			Gravity sliding and slumping following uplift
	Te_5	Non-deposition	Emplacement of ultrabasic rocks by faulting		Strong folding, faulting, and uplift
OLIGOCENE	Te_{1-4}	CROCKER FORMATION : sandstone, siltstone, red and grey shale and mudstone		26	Infilling of eugeosynclinal trough
	Tcd			38	
EOCENE	Tb	TRUSMADI FORMATION : grey and dark grey argillite, slate, siltstone and sandstone	Intermittent spilite lavas		Eugeosynclinal, flysch-type deposition
PALAEOCENE	Ta			54	
UPPER CRETACEOUS		(CHERT-SPILITE FORMATION : chert, greywacke, limestone)	(Basic intrusive and extrusive rocks : mainly spilite and sodic dolerite)	65	
			Intrusion of ultrabasic rocks at depth	100	Initiation of eugeosynclinal trough
LOWER CRETACEOUS		Non-depositon			
TRIASSIC-JURASSIC OR OLDER		CRYSTALLINE BASEMENT : schist, gneiss		136	Deposition, folding, and metamorphism of the Crystalline Basement. Possibly two cycles of intrusion

(taken from Newton-Smith, J., 1967)

2-3 Result of the Survey

2-3-1 Investigation of Locality of Mineral Occurrence

Twenty-eight localities of mineral occurrence of Cyprus-type massive, networked, and disseminated iron sulfide embedded in basalt and some dolerite of the ophiolite complex, namely 13 localities in the Bidu Bidu Hills area; 1 in East Sualog, 2 in Kiabau, 3 in Porog, 3 in Southwest Sualog, 1 in Ulu West Sualog, 3 in West Sualog; and 15 localities in the Telupid area; 1 (Tg-1) at the riverside of the S. Unsadan, a tributary of the S. Tungud, 1 (E-1) at the roadside in the upper basin of the S. Ensuan, 1 (TE-1) at the Forestry Training Institute site in Telupid, 11 (ST-2 ~ ST-6, ST-9 ~ ST-13, ST-15) along the S. Telupid to the southwest of Telupid, 1 (Kg-2) at the riverside of the S. Karang, a tributary of the S. Karamuak, were investigated.

The result of the investigation is summarized in the Table II-2-3 and the locations of the localities of mineral occurrence are shown in the Fig. II-2-1 attached at the end of this report.

The results of the chemical analysis and microscopic observation of ore samples taken at the localities of mineral occurrence are given in the Table II-2-9 in the following section 2-4 and in the Table II-2-7 in the section 2-3-2-(5) respectively.

The results of the chemical analysis and microscopic observation of the representative rock samples taken at and around the localities of mineral occurrence are given in the Table II-2-5 in the following section 2-3-2-(2) and in the Table 2-2-6 in the section 2-3-2-(3) respectively.

The result of the investigation of the main localities of mineral occurrence except for known ore deposits and mineral occurrences is summarized below.

(1) Sungai Telupid area (ST-2 ~ ST-6, ST-9 ~ ST-13, ST-15)

Eleven localilties of mineral occurrence of the massive, lenticular, veined, networked, and disseminated mineralized zone of Cyprus-type cupriferous iron sulfide, which consists mainly of pyrite, limonite, quartz, and chalcopyrite with minor amounts of bornite, chalcocite, covellite, malachite, sphalerite, and magnetite in places, in basalt and some dolerite of the ophiolite complex are found along the Sungai Telupid, situated about 6 kilometers west-northwest of Telupid, for a distance of about 160 meters. The whole mineralized zone can be regarded as a network ore body with a length of about 155 meters in the direction of the northeast and a width of about 15 meters.

The assay result of 14 ore samples taken at 11 localities of mineral occurrence reveals that the ore samples from 6 localities contain copper over 0.5% (0.88% ~ 11.05%).

As shown in the Table II-2-5, the ore samples taken at 7 localities of mineral occurrence out of 11 localities consist mainly of a large to middle amount of pyrite, a large to middle amount of quartz, and a middle to minor amount of chalcopyrite, accompanied, in places, by a trace of bornite, chalcocite, covellite, sphalerite, a middle to trace of magnetite, and a middle to trace of hematite.

Basalt and some dolerite in which the mineralized zone is embedded have been subjected to chloritization and partial epidotization.

(2) Porog area (Po-1, Po-2, Po-3)

Two outcrops (Po-2, Po-3) and floats (Po-1) of massive gossan consisting of limonite and hematite are found around Kg. Porog to the north of Kg. Kiabau in the Bidu Bidu Hills area.

Floats at the Po-1 locality are found at the ridge and slope of the hill and those at the ridge can be nearly regarded as a outcrop. The Po-2 locality is a outcrop, six meters wide, at the roadside. Four exposures of massive gossan (an area of 3.5 m × 2.0 m, 5.3 m × 4.4 m, 6.2 m × 5.4 m, 3.0 m × 2.0 m) are found at the riverbed of S. Porog for a distance of 71 meters.

These massive gossans consist of yellowish brown limonite and red or steel blue hematite.

Massive gossans at three localities of mineral occurrence consist of limonite, quartz, and hematite under a microscope and contain 55.58 to 58.34% of Fe and 0.11 to 0.40% of Cu which still remain in gossans.

These massive gossans are considerably similar to those which are found at the surface of Cyprus-type massive cupriferous iron sulfide deposits of West Sualog and Kiabau in the Bidu bidu Hills area in point of the megascopic observation, microscopic observation, and assay result. Therefore, massive gossans at 3 localities seem to have been formed by oxidation of Cyprus-type massive cupriferous iron sulfide body near the surface.

(3) S. Tungud area (Tg-1)

The semi-massive, networked, and disseminated mineralized zone of Cyprus-type cupriferous iron sulfide, which consists of pyrite, limonite, quartz, and a

small amount of chalcopyrite and is 20 meters long and 8 meters high, in metadolerite of the ophiolite complex are exposed along the S. Unsadan, a tributary of the S. Tungud, situated about 30 kilometers north-northwest of Telupid.

One of two ore samples contains 0.27% of copper and consists of a large quantity of quartz, a middle quantity of pyrite, and a trace of chalcopyrite under a ore microscope.

It is reported by Yan (1987) that high Cu·Zn anomalies of the geochemical surveys by the use of stream sediment, conducted by the Malaysia-Germany exploration project for 1980 to 1984 and by the base metal exploration project of Geological Survey of Malaysia for 1986 to 1990, were detected in the upper basin of the S. Unsadan including the Tg-1 mineralized zone.

Table II-2-3 List of Localities of Mineral Occurrence Investigated in Labuk Region

Region	Locality Name	Locality Number	Mineral Assemblage	Occurrence	Strike & Dip	Size of Orebody (in meter)	Host Rock	Alteration of Host Rock	Sample No.
Labuk	East Sualog	ES-3	py·lim	semi-massive~disseminated	—	L=3.6, H=1.5	pillow basalt	chloritization	ES-3-0
"	Ensuan	E-1	py·lim+qz·cp	massive~semi-massive~disseminated	—	L=2.2, W=0.1~1.5	pillow basalt	chloritization	E-1-0
"	Karang	Kg-2	lim	semi-massive	N50°E·75°S	H=3.0+, W=2.6	pillow basalt	chloritization	Kg-2-0
"	Kiabau	KB-1**	hm+lim	boulder of massive gossan	—	max. D=0.5	—	—	KB-1-0
"	"	KB-3	qz+lim	vein along joint	N70°E·75°N	L=1.2, W=0.02~0.06	dolerite	choritization	KB-3-0
"	Porog	Po-1**	hm	boulder of massive gossan	—	max. 1.0×0.5	—	—	Po-1-0
"	"	Po-2	hm·lim	massive gossan	N10°W·60°E	L=5.0+, W=6.0	?	?	Po-2-0
"	"	Po-3	hm·lim	massive gossan	N50°W·?	L=71.0+, W=5.5+	?	?	Po-3-0
"	Southwest Sualog	SW-1	qz+hm·lim·py·cp	vein~lenticular~disseminated	N45°E·?	L=4.8, W=0.1~0.75	basalt	chloritization	SW-1-0
"	"	SW-5	py·lim+qz	disseminated~lenticular	—	0.15×0.10×0.10	pillow basalt	chloritization, silicification	SW-5-0
"	"	SW-6	qz+py·lim·sp+cp	network	N22°W·?	L=5.0, W=0.2~0.45	pillow basalt	chloritization	SW-6-0-1 SW-6-0-2
"	Sungai Telupid	ST-2	py·lim+qz	vein	N20°E·90°	L=4.5, W=0.06~0.1	pillow basalt	chloritization, epidotization	ST-2-0
"	"	ST-3	py·lim·qz	network & lenticular	—	L=3.9+, W=5.0	pillow basalt	chloritization, epidotization	ST-3-0-1 ST-3-0-2
"	"	ST-4	qz+lim·py	vein	N50°E·?	L=1.0, W=0.05~0.25	pillow basalt	chloritization	ST-4-0
"	"	ST-5	py·lim+qz·cp	lenticular	—	L=1.0, W=0.7	pillow basalt	chloritization	ST-5-0
"	"	ST-6	py·lim+qz·cp·bo	vein	N40°E·76°W	L=1.8, W=0.05~0.1	pillow basalt	chloritization	ST-6-0
"	"	ST-9	py·lim+cp·qz	network	N16°~26°E·90°	L=5.5, W=0.5~1.3	metadolerite	chloritization, epidotization	ST-9-0
"	"	ST-10	py+qz·lim+cp	vein~lenticular	N60°E·90°	L=2.5, W=0.05~0.4	basalt	chloritization	ST-10-0
"	"	ST-11	lim·py·qz	vein	N60°E·90°	L=4.0, W=0.1~0.2	basalt	chloritization	ST-11-0-1
			py·lim+cp·qz	vein	N60°E·90°	L=9.5, W=0.05~0.2	basalt	chloritization	ST-11-0-2
"	"	ST-12	py·lim+qz+cp	network & lenticular	N50°E·?	L=20.0, W=0.2~5.0	basalt	chloritization	ST-12-0-1
			py·lim+qz	network & lenticular					ST-12-0-2
"	"	ST-13	qz+lim·py·cp·mal	network	N40°E·?	L=13.5, W=2.0~4.5	basalt	chloritization, epidotization	ST-13-0

Region	Locality Name	Locality Number	Mineral Assemblage	Occurrence	Strike & Dip	Size of Orebody (in meter)	Host Rock	Alteration of Host Rock	Sample No.
Labuk	Sungai Telupid	ST-15	qz+mt·lim·py·cp·bo·mal	network	E-W·?	L=10.0, W=1.0~4.0	basalt	chloritization, epidotization	ST-15-0
"	Telupid	TE-1	qz+py·cp	vein and disseminated	N12°W·72°E	L=0.8, W=0.02~0.05	basalt	chloritization	TE-1-0
"	Tungud	Tg-1	py·lim·cp	network, semi-massive, disseminated	N60°W·?	L=20.0+, H=8.0+	metadolerite	chloritization	Tg-1-0-1 Tg-1-0-2
"	Ulu West Sualog	UWS-2	qz+py·lim·cp	network	E-W·?	L=6.5, W=1.5	altered pillow basalt	chloritization, epidotization	UWS-2-0
"	West Sualog	WS-3	py·lim	lenticular	—	L=0.2, W=0.1	pillow basalt	chloritization	WS-3-0
"	"	WS-4**	hm·lim	boulder of massive gossan	—	max. 3.0×2.0×1.0	—	—	WS-4-0
"	"	WS-5	hm+lim	massive gossan	N30°E·?	L=18.0, W=1.3~3.0	—	—	WS-5-0

Abbreviations:
**: boulder of gossan nearly in situ, py: pyrite, cp: chalcopyrite, bo: bornite, hm: hematite, lim: limonite, mal: malachite, qz: quartz, sp: sphalerite, mt: magnetite, max.: maximum, L: length, W: width, H: height, D: diameter, 6.0+: 6.0 and over

2-3-2 Laboratory Work

(1) K-Ar age determination of rock (11 samples)

Eleven representative rock samples, namely 4 samples of basalt, 5 samples of dolerite, and 2 samples of gabbro in the ophiolite complex, out of 32 rock samples taken at and near the localities of mineral occurrence in the Bidu Bidu Hills and Telupid areas for the microscopic observation and chemical analysis, were dated by means of the K-Ar method of whole rock.

The result is shown in the Table II-2-4. As shown in the Table II-2-4, 3 samples of basalt (E-1-D, TE-1-d, WS-2-D) and 5 samples of dolerite (ES-1-D, KB-2-D, SW-2-D, SP-1-D, Tg-1-D) have been dated as 26.6±8.1 Ma (Late Oligocene) to 40.5±4.2 Ma (Late Eocene). The age of the sample Kg-1-D of gabbro has been determined as 13.1±2.0 Ma on the average (Middle Miocene) and is younger than those of the above 8 samples. The sample ST-1-D of basalt has been dated as 123±63 Ma on the average (Early Cretaceous) and is older than the said samples in age. The age of the sample UWS-1-D of gabbro has been determined as 248.5±116 Ma on the average (Latest Permian) and is oldest among 20 samples (including 9 samples taken in the Kinabalu region) dated.

The result of the age determination indicates that basalt and dolerite, in which Cyprus type massive, networked, and disseminated cupriferous iron sulfide is embedded, in the ophiolite complex have been mostly dated as 26.6±8.1 ~ 40.5±4.2 Ma (8 samples out of 9 samples), except for 1 sample (ST-1-D) which has been dated with big error due to a very low content of K_2O in the samples (0.01% K_2O).

Table II-2-4 Result of K-Ar Dating of Basic Igneous Rock in Labuk Region

Locality Name	Sample Number	Numbers in Laboratory	Sample Type	Potassium (K wt%)	Rad. ^{40}Ar (10^{-6}cc/g)	K-Ar Age (Ma)	Air Cont. (%)
East Sualog	ES-1-D	SH5-226 -227	Whole Rock (Dolerite)	0.10 ±0.02	13.3±0.5 12.4±0.5	33.9 ±6.9 31.8 ±6.4 Avg. 32.85±6.65	68.1 69.7
Ensuan	E-1-D	SH5-228 -229	Whole Rock (Basalt)	0.38 ±0.04	53.2±1.0 53.9±0.9	35.7 ±3.6 36.2 ±3.6 Avg. 35.95±3.6	37.2 34.1
Karang	Kg-1-D	SH5-230 -231	Whole Rock (Gabbro)	0.27 ±0.04	13.7±0.5 13.9±0.5	13.0 ±2.0 13.2 ±2.0 Avg. 13.1 ±2.0	64.9 63.6
Kiabau	KB-2-D	SH5-232 -233	Whole Rock (Dolerite)	0.18 ±0.04	24.2±0.7 25.0±0.7	34.3 ±6.9 35.4 ±7.1 Avg. 34.85±7.0	55.5 54.4
Southwest Sualog	SW-2-D	SH5-234 -235	Whole Rock (Dolerite)	0.34 ±0.03	54.0±1.6 52.2±1.4	40.5 ±4.2 39.2 ±4.0 Avg. 39.85±4.1	59.5 55.8
Sualog/Pari	SP-1-D	SH5-236 -237	Whole Rock (Metadolerite)	0.08 ±0.02	9.11±0.69 8.32±0.58	29.1 ±8.9 26.6 ±8.1 Avg. 27.85±8.5	80.0 80.9
Sungai Telupid	ST-1-D	SH5-238 -239	Whole Rock (Altered basalt)	0.01 ±0.005	5.39±1.09 4.47±0.74	134 ± 69 112 ± 57 Avg. 123 ± 63	92.3 91.3
Telupid	TE-1-D	SH5-240 -241	Whole Rock (Altered basalt)	0.19 ±0.04	21.0±0.6 20.6±0.6	28.3 ±5.7 27.8 ±5.6 Avg. 28.05±5.65	57.3 57.9
Tungud	Tg-1-D	SH5-242 -243	Whole Rock (Metadolerite)	0.11 ±0.02	13.2±0.6 13.3±0.6	30.6 ±6.2 30.8 ±6.2 Avg. 30.7 ±6.2	69.7 70.0
Ulu West Sualog	UWS-1-D	SH5-244 -245	Whole Rock (Gabbro)	0.01 ±0.005	10.4±0.5 10.2±0.5	251 ±117 246 ±115 Avg. 248.5±116	71.1 71.6
West Sualog	WS-2-D	SH5-246 -247	Whole Rock (Altered basalt)	0.49 ±0.05	52.6±0.8 52.4±0.6	27.4 ±2.76 27.3 ±2.75 Avg. 27.35±2.75	32.8 32.4

(2) Chemical analysis of rock (32 samples)

The assay result of 32 rock samples, namely 11 samples taken at the same localities as the samples for the K-Ar age determination, 7 samples of basalt, 3 samples of dolerite, 2 samples of gabbro, and 9 samples of ultrabasic rock in the ophiolite complex, is shown in the Table II-2-5.

The analyses of 19 samples, namely 11 samples of basalt and 8 samples of dolerite, out of 32 rock samples analyzed chemically, have been plotted on the following several diagrams for the petrological study.

At first, the analyses of SiO_2 and Na_2O+K_2O have been plotted on the SiO_2-Na_2O+K_2O diagram and the result is given in the Fig. II-2-6. The Fig. II-2-6 shows that the samples of basalt and dolerite have been plotted within every field of the alkali basalt, high alkali tholeiite, and low alkali tholeiite after Kuno (1968).

Secondly, MFA trigonal diagram of the Fig. II-2-7, on which the analyses of MgO, Na_2O+K_2O, and FeO* calculated as total FeO from the analyses of FeO and Fe_2O_3 have been plotted, the SiO_2-FeO*/MgO diagram of the Fig. II-2-8, and the FeO-FeO*/MgO diagram of the Fig. II-2-9 show that the samples of basalt and dolerite have been plotted in both the fields of tholeiite and calc-alkali series after Irvine and Barager (1971) and Miyashiro (1974).

Next, the TiO_2-FeO*/MgO diagram of the Fig. II-2-10 indicates that all samples except the sample ST-1-R (basalt) have been plotted within the field of MORB (Mid-ocean ridge basalt) after Shimazu et al. (1990).

At last, the Al_2O_3-TiO_2 diagram of the Fig. II-2-11 shows that 12 samples have been plotted within the field of MORB after Aoki and Ito (1968) and 2 samples belong to OIT (Oceanic island tholeiite) with 3 samples within the overlapping field of MORB and OIT; that is, 15 samples out of 19 samples belong to MORB.

The petrological study by the use of the above several diagrams reveals that basalt and dolerite, which constitute the ophiolite complex and host Cyprus type cupriferous iron sulfide ore, have been mainly plotted within the field of MORB and consist of alkali basalt, tholeiite, and calc-alkali rock series.

Table II-2-5 Assay Result of Rock Samples taken in Labuk Region

Locality	Sample Number	Rock Name	SiO_2 %	TiO_2 %	Al_2O_3 %	Fe_2O_3 %	FeO %	MnO %	MgO %	CaO %	Na_2O %	K_2O %	P_2O_5 %	Ig-los %	Total	Au ppb	Ag ppm	Co ppm	Cr ppm	Cu ppm	Mo ppm	Ni ppm	Pb ppm	S %	Zn ppm
Cr-1	Cr-1-R	Serpentinized Harzburgite	36.13	0.01	0.59	8.13	0.37	0.11	36.97	0.71	0.10	<0.01	0.02	16.16	99.31	<1	<0.5	84	1,067	22	<1	1,728	<1	0.034	38
ES-1	ES-A-R	Dolerite	51.15	1.15	15.39	1.99	6.92	0.19	7.79	10.65	2.68	0.11	0.10	1.39	99.51	<1	0.6	41	200	11	<1	71	8	0.062	36
ES-2	ES-2-R	Serpentinized Lherzolite	40.58	0.10	2.58	5.58	2.51	0.14	35.97	2.05	0.09	0.01	0.03	10.00	99.64	67	<0.5	82	1,360	20	<1	1,601	<1	0.062	38
ES-3	ES-3-R	Altered Basalt	53.83	1.46	14.38	4.20	6.36	0.16	7.82	1.61	4.18	0.02	0.17	5.26	99.45	<1	<0.5	27	70	15	<1	27	9	2.204	113
E-1	E-1-R	Basalt	47.97	1.41	13.95	5.32	5.66	0.18	6.00	10.50	3.81	0.64	0.16	4.02	99.62	<1	0.6	44	214	58	<1	83	6	0.075	84
Ga-1	Ga-1-R	Serpentinized Harzburgite	42.04	0.03	0.95	2.90	5.09	0.12	41.64	1.15	0.02	<0.01	0.03	5.23	99.21	2	<0.5	90	1,071	13	<1	1,819	2	0.028	39
Kr-1	Kr-1-R	Serpentinized Wehrlite	36.46	0.02	6.03	3.99	3.90	0.11	30.85	7.24	0.08	<0.01	0.03	10.71	99.43	13	<0.5	79	458	57	<1	1,616	37	0.071	37
Kg-1	Kg-1-R	Gabbro	48.51	0.57	16.69	1.77	6.03	0.14	7.76	10.20	3.80	0.26	0.03	3.47	99.23	<1	<0.5	29	119	23	<1	38	8	0.593	44
KB-2	KB-2-R	Dolerite	47.66	0.93	16.38	2.12	5.72	0.25	8.71	9.11	3.59	0.19	0.09	4.65	99.40	<1	0.5	39	268	172	<1	86	8	0.449	829
KB-3	KB-3-R	Dolerite	49.75	1.30	15.05	2.53	6.60	0.23	7.46	7.46	4.85	0.29	0.13	3.88	99.53	<1	<0.5	39	142	77	<1	50	11	0.448	128
Po-2	Po-2-R	Serpentinized Lherzolite	41.45	0.11	2.26	4.09	3.90	0.12	36.59	2.52	0.03	<0.01	0.03	8.23	99.34	<1	<0.5	86	1,089	18	<1	1,643	<1	0.103	45
Pm-1	Pm-1-R	Serpentinized Harzburgite	36.11	0.01	0.44	6.16	1.13	0.10	37.39	0.74	0.01	<0.01	0.03	17.47	99.60	3	<0.5	83	868	13	<1	1,659	1	0.085	39
SW-1	SW-1-R	Basalt	53.64	1.21	15.54	3.75	3.77	0.26	6.89	4.15	5.74	0.01	0.08	4.26	99.30	<1	0.8	31	315	1,129	<1	87	11	0.465	665
SW-2	SW-2-R	Dolerite	48.52	0.71	15.55	4.33	3.27	0.30	11.14	6.09	4.20	0.21	0.07	5.01	99.40	<1	<0.5	39	308	183	<1	120	12	0.159	103
SW-3	SW-3-R	Metagabbro	47.77	0.20	17.48	4.60	2.01	0.10	11.36	13.15	1.32	0.06	0.03	1.21	99.29	<1	<0.5	36	485	19	<1	193	7	0.067	29
SW-4	SW-4-R	Serpentinite	37.50	0.06	1.53	10.08	0.13	0.09	36.04	0.06	<0.01	<0.01	0.03	13.52	99.06	<1	<0.5	104	2,783	4	<1	2,257	<1	0.010	50
SW-5	SW-5-R	Basalt	64.41	1.05	12.55	8.52	0.26	0.01	0.45	1.16	4.16	0.10	0.09	6.69	99.45	103	11.4	40	279	58	19	95	69	4.557	253
SW-6	SW-6-R	Basalt	47.90	0.98	16.54	2.64	5.16	0.35	10.00	7.12	3.50	0.06	0.11	4.91	99.27	2	0.7	38	228	63	<1	125	10	0.215	78
SW-7	SW-7-R	Serpentinized Lherzolite	39.69	0.09	3.01	8.65	0.13	0.14	33.19	1.83	0.03	<0.01	0.03	12.70	99.50	9	<0.5	87	1,151	24	<1	1,620	3	0.033	43
SP-1	SP-1-R	Metadolerite	48.36	1.02	14.68	4.42	4.90	0.16	8.24	8.99	3.57	0.07	0.10	5.22	99.73	2	<0.5	39	90	38	<1	51	4	0.070	56
ST-1	ST-1-R	Altered Basalt	49.68	0.35	14.61	3.82	4.34	0.19	10.40	7.54	3.93	0.01	0.03	4.52	99.42	<1	<0.5	33	292	87	<1	85	9	0.074	89
ST-7	ST-7-R	Metagabbro	48.56	0.35	18.52	3.82	0.31	0.07	6.91	14.13	2.86	0.15	0.04	3.95	99.67	1	<0.5	21	406	85	<1	133	9	0.078	19
ST-8	ST-8-R	Metadolerite	49.18	1.09	15.65	1.77	7.10	0.20	9.20	7.09	4.08	0.26	0.11	3.62	99.35	<1	0.6	40	260	15	<1	89	4	0.064	80
ST-9	ST-9-R	Metadolerite	52.04	2.05	13.86	4.37	8.49	0.27	5.21	5.83	4.06	0.20	0.22	2.77	99.37	<1	0.7	48	65	87	<1	23	5	0.253	132
ST-14	ST-14-R	Basalt	50.76	0.98	15.75	2.54	6.03	0.21	8.11	7.45	4.58	0.18	0.10	3.04	99.73	2	0.6	38	129	70	<1	51	5	0.288	113
TE-1	TE-1-R	Altered Basalt	47.94	1.09	15.19	3.16	5.91	0.22	9.27	6.77	3.65	0.46	0.11	5.84	99.61	2	<0.5	38	214	5	<1	66	6	0.061	79
Tg-1	Tg-1-R	Metadolerite	51.85	1.67	14.82	4.89	6.79	0.30	5.54	8.46	3.05	0.13	0.17	2.03	99.70	<1	0.5	47	61	102	<1	27	9	0.143	101
UP-1	UP-1-R	Serpentinite	38.74	0.01	0.08	8.78	0.13	0.25	36.04	0.07	0.01	<0.01	0.03	14.02	99.17	6	<0.5	116	12,930	3	<1	3,219	2	0.010	44
UWS-1	UWS-1-R	Gabbro	47.49	0.16	16.13	1.16	6.41	0.13	14.73	10.96	1.71	0.01	0.03	0.60	99.52	1	<0.5	55	369	64	<1	310	9	0.081	39
UWS-2	UWS-2-R	Altered Basalt	56.69	1.87	12.89	5.48	5.29	0.27	6.53	2.20	3.37	0.01	0.18	4.86	99.64	<1	0.6	39	102	56	<1	10	6	2.529	212
WS-2	WS-2-R	Altered Basalt	46.57	1.05	15.61	5.35	2.77	0.17	7.96	10.31	2.75	0.54	0.11	6.23	99.42	<1	<0.5	39	253	41	<1	80	11	0.054	61
WS-3	ES-3-R	Basalt	50.58	1.24	15.93	3.60	4.40	0.15	8.45	3.73	5.27	0.07	0.12	5.98	99.52	2	0.6	36	220	46	<1	71	5	0.342	86

Figure II-2-6 $Na_2O + K_2O$ - SiO_2 Diagram of Basalt and Dolerite of Ophiolite Complex in Labuk Region

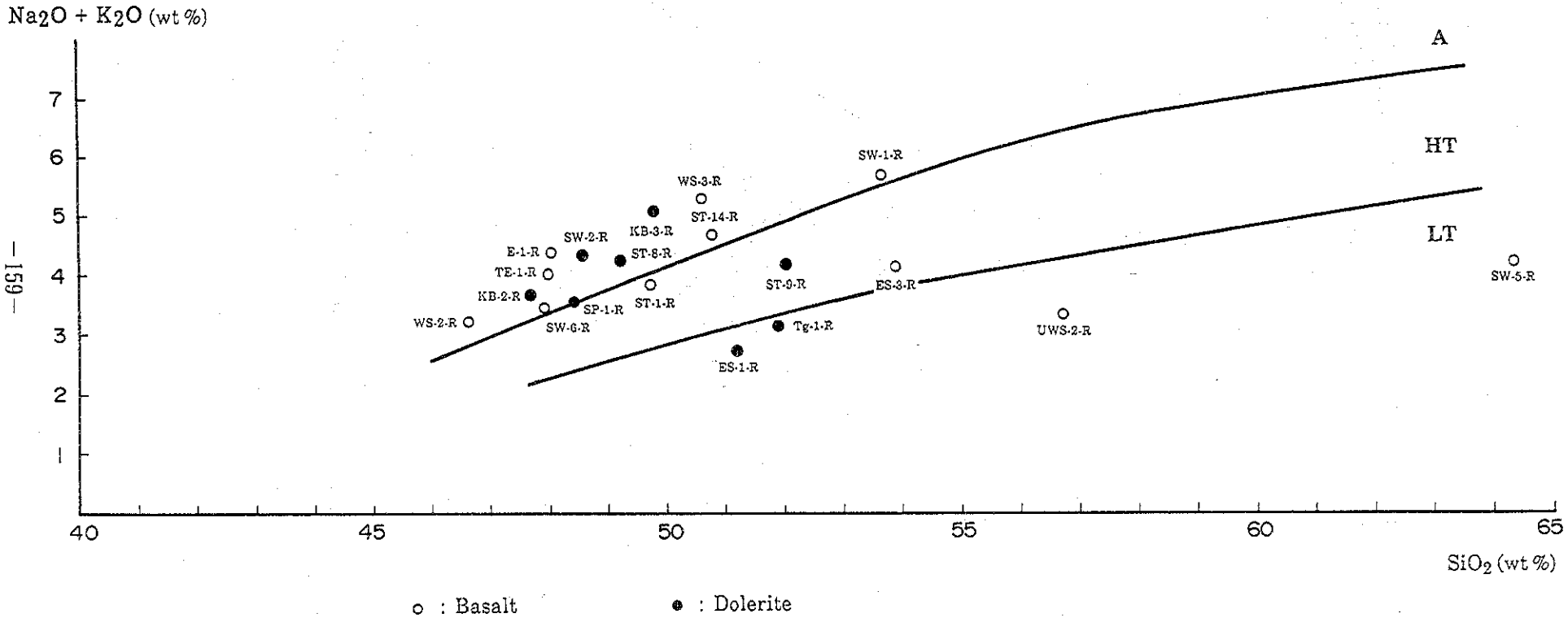

A: Alkali basalt series; HT: High alkali tholeiite series, LT: Low alkali tholeiite series (after Kuno 1968)

Figure II-2-7 $FeO + Fe_2O_3$ - $Na_2O + K_2O$ - MgO Trigonal Diagram (MFA Diagram) of Basalt and Dolerite of Ophiolite Complex in Labuk Region

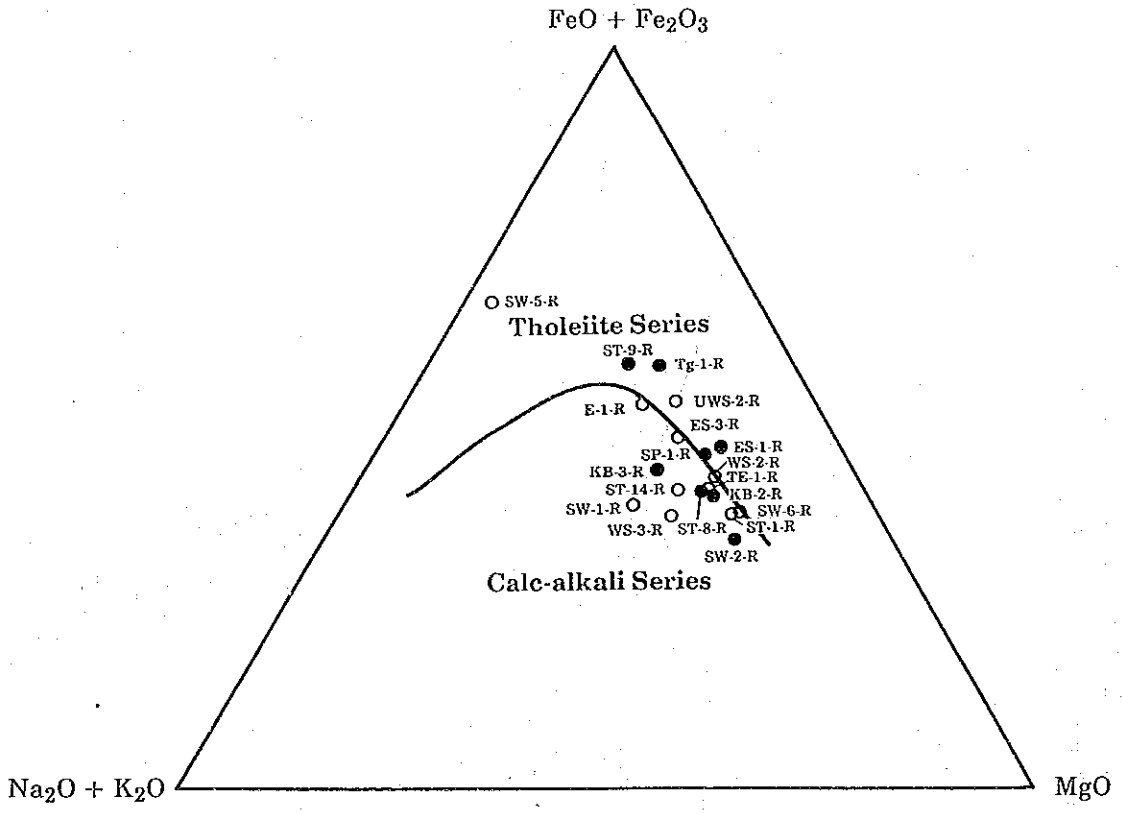

o : Basalt ● : Dolerite

Solid line is boundary between tholeiite series and calc-alkali series after Irvine and Barager (1971)

Figure II-2-8 SiO_2 - FeO*/MgO Diagram of Basalt and Dolerite of Ophiolite Complex in Labuk Region

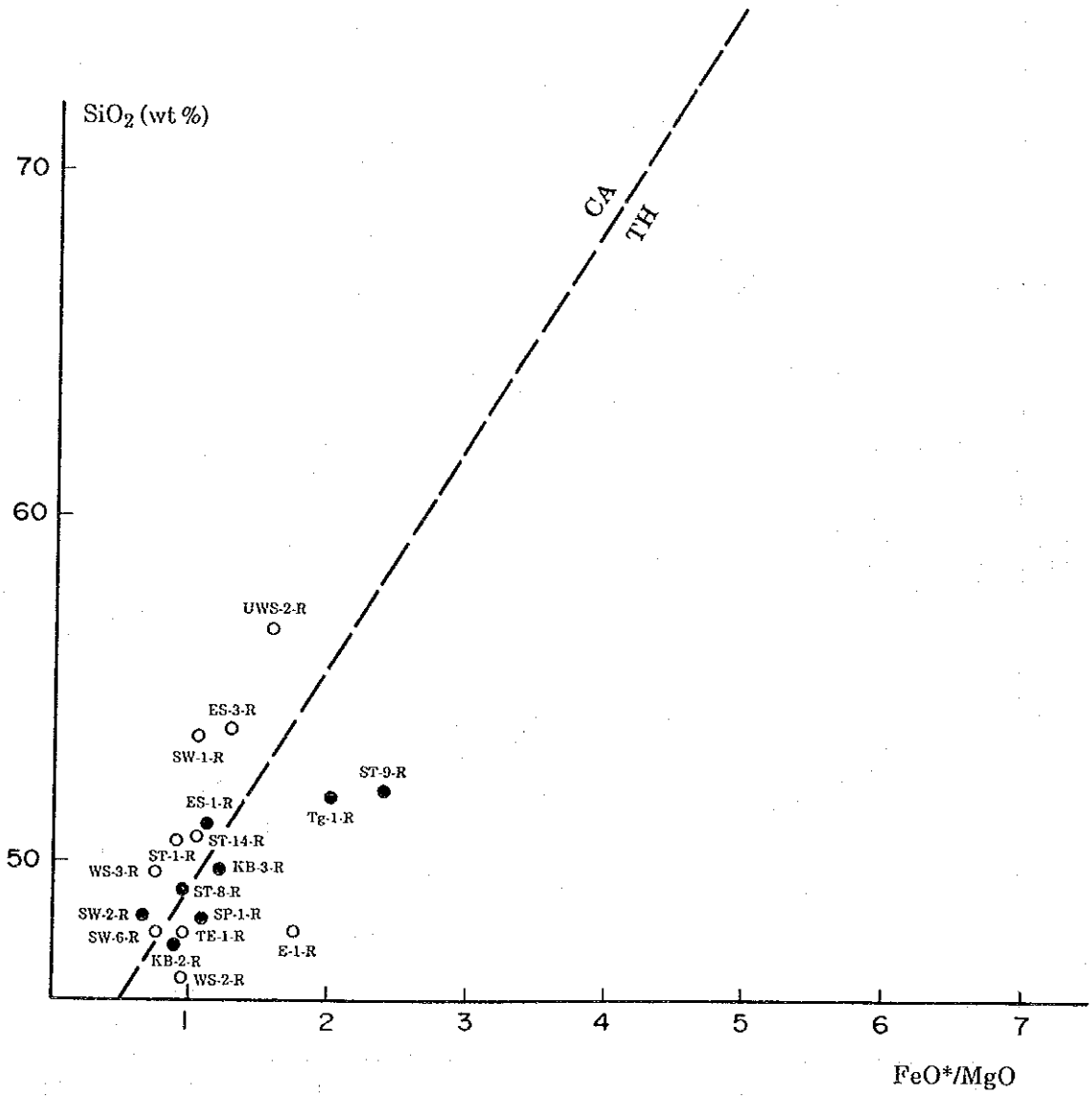

FeO*: Total Fe as FeO

○ : Basalt ● : Dolerite

TH (tholeiitic) / CA (calc-alkaline) boundary: after Miyashiro, 1974

Figure II-2-9 FeO* - FeO*/MgO Diagram of Basalt and Dolerite of Ophiolite Complex in Labuk Region

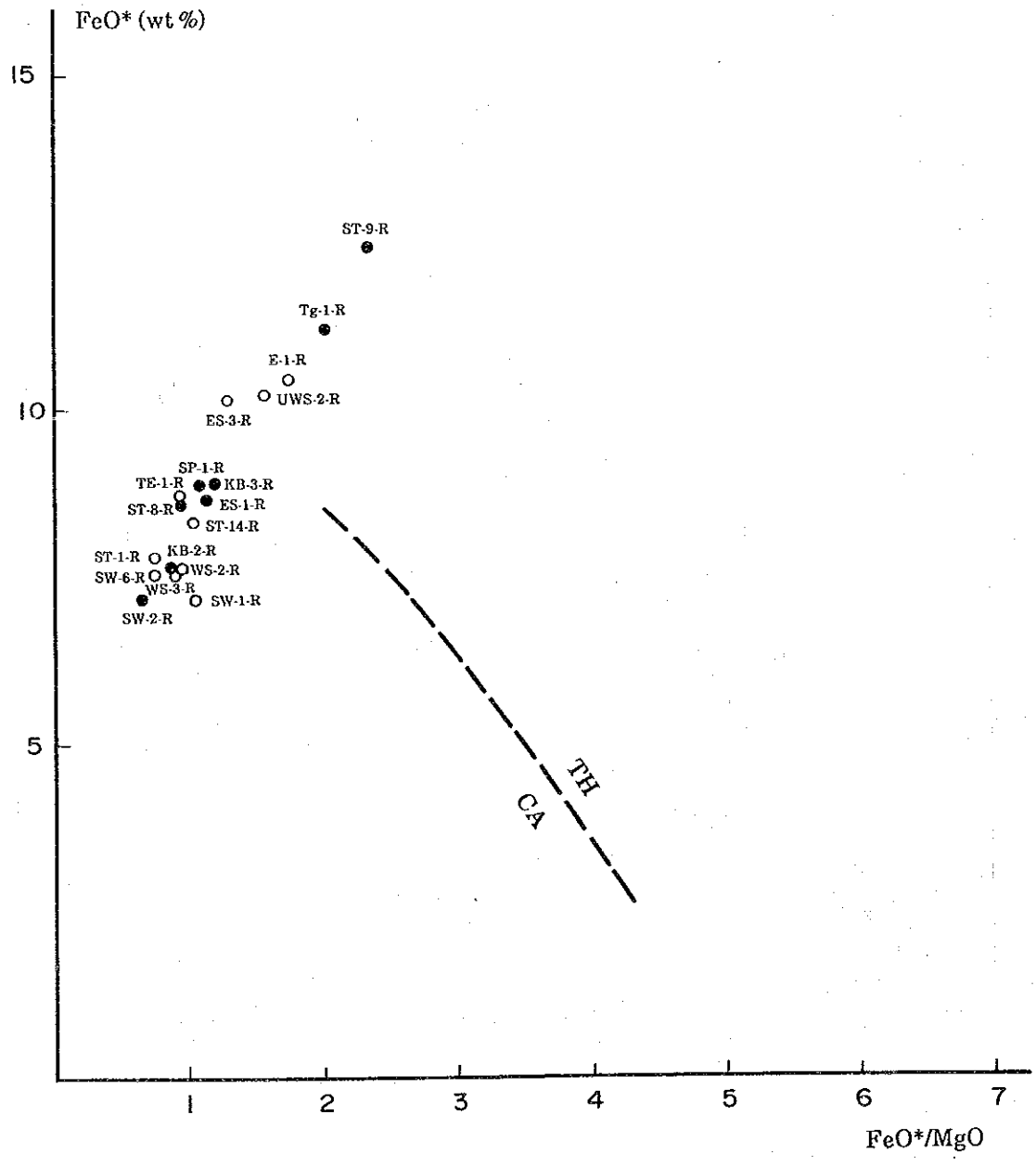

FeO*: Total Fe as FeO

○ : Basalt ● : Dolerite

TH (tholeiitic) / CA (calc-alkaline) boundary: after Miyashiro, 1974

Figure II-2-10 TiO_2 - FeO*/MgO Diagram of Basalt and Dolerite of Ophiolite Complex in Labuk Region

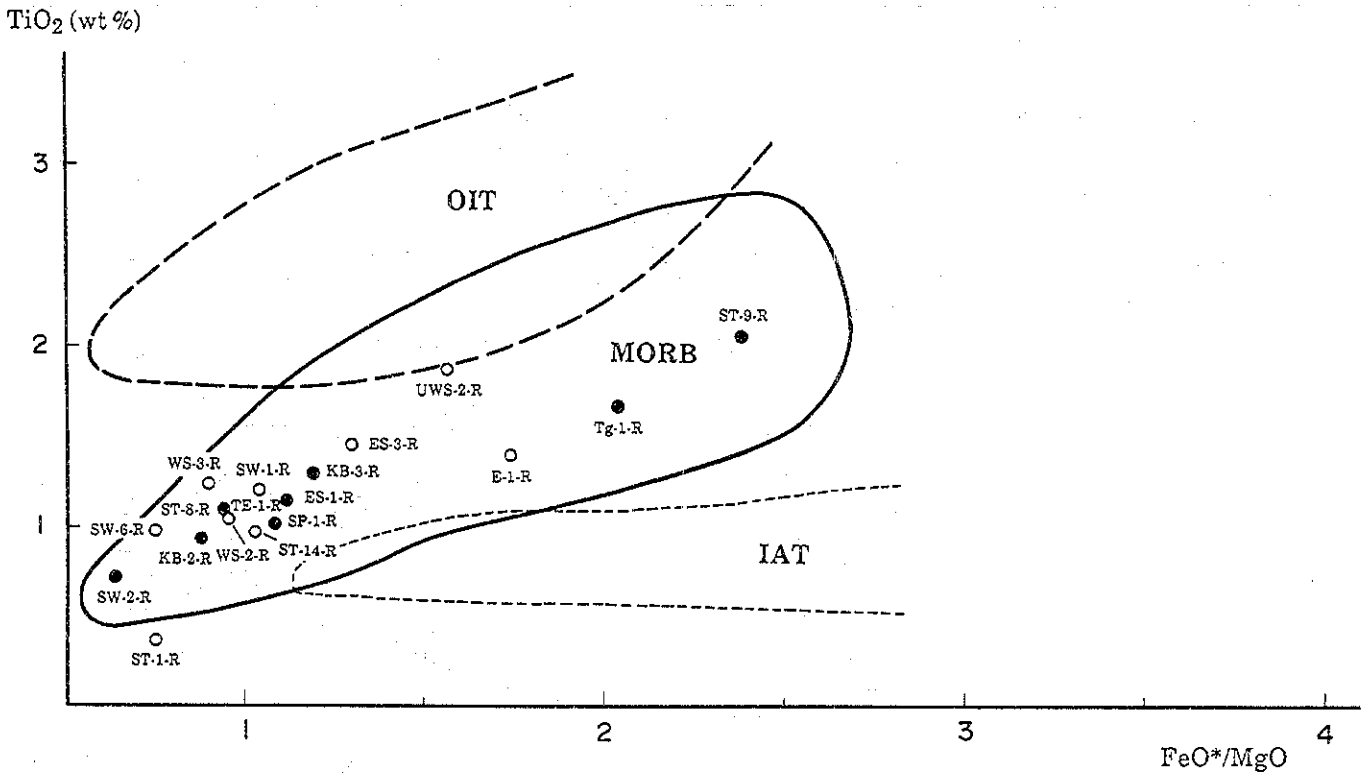

FeO*: Total Fe as FeO

○ : Basalt ● : Dolerite

MORB: Mid-ocean ridge basalt; OIT: Oceanic island tholeiite
IAT : Island arc tholeiite (after Shimazu et al., 1990)

Figure II-2-11 TiO_2 - Al_2O_3 Diagram of Basalt and Dolerite of Ophiolite Complex in Labuk Region

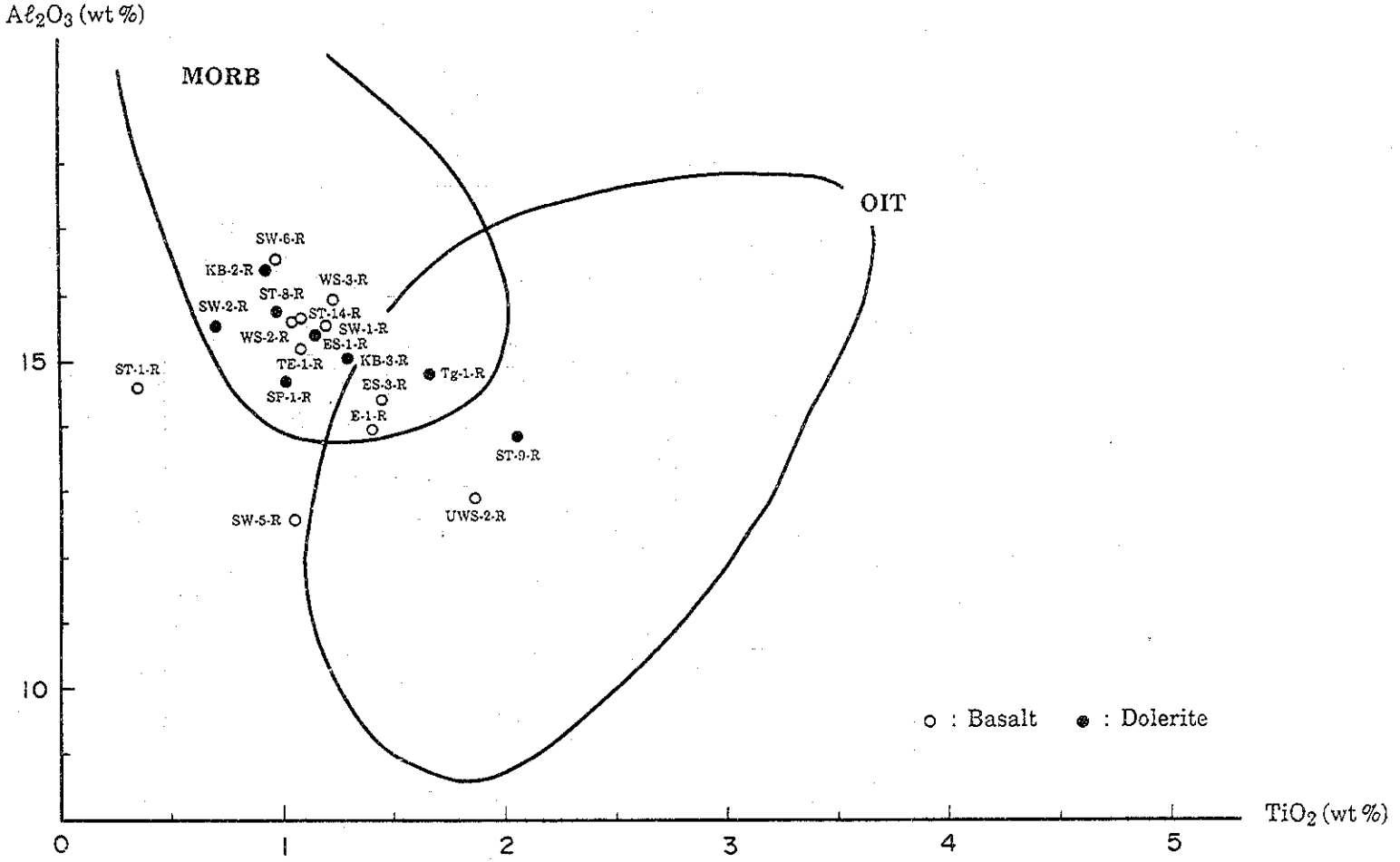

MORB: Mid-ocean ridge basalt; OIT: Oceanic island tholeiite
(after Aoki and Ito, 1968)

(3) Microscopic observation of thin section of rock (32 samples)

The thin sections made from 32 rock samples obtained at the same localities as the samples for the chemical analysis, namely 11 samples of basalt, 8 samples of dolerite, 4 samples of gabbro, and 9 samples of ultrabasic rock in the ophiolite complex, were observed under a polarization-microscope, and the result of the observation is shown in the Table II-2-6.

Table II-2-6 Result of Microscopic Observation of Thin Sections of Rock Samples taken in Labuk Region

Location	Sample Number	Rock Name	Texture	Phenocryst, Fragments									Groundmass, Matrix, Accessary Minerals										Alteration, Metamorphic Minerals											Remarks
				Quartz	Plagioclase	K-feldspar	Olivine	Augite	Hypersthene	Hornblende	Biotite	Others	Quartz	Plagioclase	K-feldspar	Augite	Hornblende	Biotite	Zircon	Apatite	Sphene	Opaque Minerals	Others	Quartz	Hornblende	Tremolite	Actinolite	Epidote	Zoisite	Biotite	Serpentine	Chlorite	Sericite	Calcite	Kaolinite	Others	
East Sualog	Es-1-T	Dolerite	subophitic											◎		●					●	●*					◎	●				●	●				* Magnetite, equigranuler dolerite, augite is changed to actinolite.
"	Es-3-T	Basalt	aphyric intergranular		●									◎								●*		○				○				◎					* Pyrite, altered basalt, phenocryst is rare.
Ensuan	E-1-T	Brecciated basalt	pyroclastic									◎*		○		◎						●	**◎					●				○					* Basalt fragment of 1 ~ 0.5 cm, ** glass.
Kiabau	KB-2-T	Dolerite	cataclastic											◎		◎					●	●*						●	●			●					* Pyrite, hematite. Cataclastic dolerite.
"	KB-3-T	Dolerite	subophitic											◎	◎						○	×						○	●			○					equigranuler dolerite.
Southwest Sualog	Sw-1-T	Basalt	porphyritic intergranular		○									◎		○					×	×						●				○	●				Fine grained basalt with weak alteration.
"	Sw-2-T	Dolerite	subophitic											◎		◎					×	●						●				○	×	●		●	* Zeolite, equigranular dolerite.
"	Sw-5-T	Basalt	intersertal		●									◎								●*	**◎	◎				●								***●	* Pyrite, ** glass, *** zeolite, fine basalt with quartz-pyrite vein, phenocryst is rare.
"	Sw-6-T	Basalt	porphyritic intergranular		◎			●						◎		○					●	×				●		●				○	●	●		*●	* Albite, chloritized basalt.
Sualog/Pari	Sp-1-T	Metadolerite	blastophitic		◎																×	●			◎			×				○		×		*●	* Zeolite, metamorphosed dolerite.
Sungai Telupid	ST-1-T	Basalt	porphyritic intergranular		●			●						◎		○					●	×						○				●		○			Fine grained altered basalt, alteration by epidote, calcite, chlorite.
"	ST-8-T	Meta dolerite	subophitic											◎		○					●	●	*●				○	●				○		×			* hypersthene
"	ST-9-T	Metadolerite	blastophitic											◎		●					×	○*		●			○	○				◎		●		**●	* Magnetite, ** zeolite, magnetite-rich metadolerite.
"	ST-14-T	Basalt	porphyritic subophitic		○									◎		◎					×	●*					●	○				○		●			* includes pyrite, coarse grained basalt.
Telupid	TE-1-T	Basalt	porphyritic intersertal		×			×						◎		◎					●	×		●				●				◎		●		*●	* Zeolite, altered fine grained basalt with rare phenocryst.
Tungud	Tg-1-T	Metadolerite	blastophitic											◎							●	○*					◎	●				●		●			* Magnetite, magnetite-rich metadolerite
Ulu West Sualog	UWS-2-T	Altered basalt	blastoporphyritic		●									○							●	●*		○				◎	●			◎					* Pyrite, strongly altered basalt with pyrite dissemination.
West Sualog	WS-2-T	Basalt	aphyric intergranular											◎		◎						●*										○		●		**●	* Magnetite and hematite, ** zeolite, altered aphyric basalt with amygdal filled by zeolite.
"	WS-3-T	Basalt	porphyritic intersertal		○			●						○								●*						●				◎				*●	* Albite, fine basalt with chloritization and albitization.

Location	Sample Number	Rock Name	Texture	Primary Minerals										Metamorphic, Alteration Minerals												Accessary Minerals									Remarks
				Plagioclase	Olivine	Augite	Hypersthene	Hornblende					Others	Hornblende	Cummingtonite	Actinolite	Tremolite	Epidote	Pumpellyite	Prehnite	Chlorite	Serpentine	Sericite	Calcite	Talc	Quartz	Others	Sphene	Picotite	Opaque						Others	
Chromite	Cr-1-T	Hartzburgite	mesh			×	●								●							◎			●				●	* ●							* Magnetite, serpentinized hartzburgite.
East Sualog	Es-2-T	Lherzolite	cataclastic	●	◎	○	○															◎			●				●	* ●							* Magnetite, serpentinized cataclastic lherzolite.
Gambaran	Ga-1-T	Hartzburgite	cataclastic		◎	●	○														●	●							●								Less serpentinized cataclastic harzburgite.
Karamuak	Kr-1-T	Wehrlite	mesh	×	◎	●															●	○							×	* ●							* Magnetite,pyroxene (probably augite) remains as only pseudomorphs, serpentinized wehrlite.
Karang	Kg-1-T	Gabbro	hypidiomorphic granular	◎		◎	●	●								●	●				●		○							●							plagioclase is saussuritized.
Porog	Po-2-T	Lherzolite	mesh	●	◎	○	○															○			●				●	* ●							* Magnetite, serpentinized lherzolite.
Pumadagan	Pm-1-T	Hartzburgite	mesh			×	* ○															◎			●				●	** ●							** Only pseudomorph remains, ** magnetite, serpentinized hartzburgite
Southwest Sualog	Sw-3-T	Metagabbro	hypidiomorphic granular	◎	●	○	●							●			●		◎		●				×					×							
"	SW-4-T	Serpentinite	mesh																			◎							×	* ○							* Magnetite,completely serpentinized.
"	SW-7-T	Lherzolite	mesh		●	○	○										●				●	◎			●				×	* ●							* Magnetite, hematite, serpentinized lherzolite.
Sungai Telupid	ST-7-T	Metagabbro	hypidiomorphic granular	◎		○	○	●							○		●	●		○	●						* ●	●		×							* Zoisite, metamorphosed coarse grained gabbro, plagioclase is saussuritized.
Ulu Pari	UP-1-T	Serpentinite	mesh																			◎								* ●							* Magnetite and hematite, completely serpentinized.
Ulu West Sualog	UWS-1-T	Gabbro	hypidiomorphic granular	◎	●	◎	●							×							×	×								×							Coarse gabbro

[Notes] ◎: Abundant, ○: Common, ●: Rare, ×: Trace

(4) Assay of ore (46 samples)

The assay result of 46 samples taken in the Bidu Bidu Hills and Telupid areas, namely 34 ore samples obtained at 28 localities of mineral occurrence of Cyprus type massive, networked, and disseminated cupriferous iron sulfide investigated and 12 samples of Cr-Ni-bearing laterite formed by the weathering of ultrabasic rock, is shown in the Table II-2-8 and Table II-2-9 in the following section 1-4.

(5) Microscopic observation of polished section of ore (23 samples)

The polished sections made from the ore samples obtained at 23 localities, out of 34 ore samples taken for assay at 28 localities of mineral occurrence of massive, networked, and disseminated Cyprus type cupriferous iron sulfide, were observed under a ore microscope. The result of the observation is shown in the Table II-2-7.

The Table II-2-7 shows that the samples Kg-2-P, KB-1-P, Po-1-P, Po-2-P, Po-3-P SW-1-P, and WS-5-P of massive gossan consist mostly of limonite, quartz, and a trace of hematite and some samples of gossan contain a trace of pyrite in addition to the above three minerals, and that massive, networked, and disseminated cupriferous iron sulfide ores other than massive gossan are composed mainly of quartz, pyrite, and chalcopyrite, and magnetite, hematite, and very small amounts of bornite, chalcocite, covellite, and sphalerite besides these three minerals are present in some samples.

Table II-2-7 Result of Microscopic Observation of Polished Sections of Ore Samples from Labuk Region

Locality Name	Sample Number	Occurrence	Chalcopyrite (cp)	Bornite (bn)	Chalcocite (cc)	Covellite (cv)	Sphalerite (sp)	Galena (gn)	Pyrite (py)	Magnetite (mt)	Hematite (hm)	Limonite (mostly geothite)	Stibnite (sb)	Gangue minerals Q:quartz	Remarks
East Sualog	ES-3-P	Pyrite dissemination							○			·		◎	
Ensuan	E-1-P	Chalcopyrite-pyrite ore	●						◎					○	
Karang	Kg-2-P	Limonite (from oxidized outcrop?)							·		·	◎		●	
Kiabau	KB-1-P	"									·	◎		○ᵠ	
Porog	Po-1-P	"									·	◎		○ᵠ	
"	Po-2-P	"							·		·	◎		○ᵠ	
"	Po-3-P	"									·	◎		○ᵠ	
Southwest Sualog	SW-1-P	"							·		·	◎		◎ᵠ	
"	SW-5-P	Pyrite ore							◎					○ᵠ	
"	SW-6-P	Chalcopyrite-pyrite-quartz veinlet and chalcopyrite-pyrite dissemination	●	·	·	·			○					◎ᵠ	
Sungai Telupid	ST-3-P	Pyrite ore							◎	●	●			○ᵠ	magnetite in pseudomorph after hematite
"	ST-6-P	Chalcopyrite-pyrite-quartz veinlet and chalcopyrite-pyrite dissemination	○	·	·	·	·		○					◎ᵠ	
"	ST-9-P	"	○						○					◎ᵠ	
"	ST-11-P	"	●		·	·			●					◎ᵠ	
"	ST-12-P	(Chalcopyrite)-pyrite dissemination	·						○	·	·			◎ᵠ	magnetite in pseudomorph after hematite
"	ST-13-P	Chalcopyrite veinlet	·				·		·					◎	
"	ST-15-P	Chalcopyrite-pyrite ore	○						○	○	○			○ᵠ	magnetite in pseudomorph after hematite
Telupid	TE-1-P	Chalcopyrite-pyrite-quartz vein	○						○					◎ᵠ	
Tungud	Tg-1-P	Pyrite dissemination	·						○					*◎ᵠ	*jusper
Ulu West Sualog	UWS-2-P	(Chalcopyrite)-(pyrite)-quartz veinlet and (chalcopyrite)-pyrite dissemination	·						·					◎	
West Sualog	WS-1-P	Chalcopyrite-pyrite-magnetite ore	◎				·		○	○				●	massive compact ore; strata-bound cp-py-mt deposit?
"	WS-3-P	Pyrite dissemination							◎					◎	
"	WS-5-P	Limonite (from oxidized outcrop?)									·	◎		●	

[Notes] ◎: Abundant, ○: Common, ●: Rare, · : Trace

2-4 Assay Result of Ore (46 samples)

The assay result of 46 samples taken in the Bidu Bidu Hills and Telupid areas, namely 34 ore samples obtained at 28 localities of mineral occurrence of Cyprus type cupriferous iron sulfide ore and 12 samples of Cr-Ni-bearing laterite formed by weathering of ultrabasic rock, is shown in the Table II-2-8 and Table II-2-9.
The Table II-2-8 shows that 13 samples contain copper over 0.3% and the sample ST-6-0 contains 11.05% of copper which is the highest copper content among 13 samples and that 3 samples (SW-6-0-1, SW-6-0-2, WS-1-0) contain 0.58 to 2.26% of zinc and 57.9 g/t of silver is contained in the sample SW-5-0.
Table II-2-8 also reveals that iron contents of massive gossans of limonite and hematite (Kg-2-0, KB-1-0, Po-1-0, Po-2-0, Po-3-0, WS-4-0, WS-5-0) are 46.29 to 58.34% and 0.11 to 0.40% of copper still remain in the gossans.
As shown in the Table II-2-9, the assay result of laterite reveals that chromium over 1.0% and nickel over 0.4% are contained in 9 samples out of 12 samples assayed and that laterite rich in chromium contains much nickel in general.
The Table II-2-9 also reveals that the laterite samples contain 0.10 to 2.45% of manganese and Pt content is higher than Au content in the laterite samples, unit of both being expressed in terms of ppb.

Table II-2-8 List of Assay Result of Ore Samples taken in Lubuk Region

Locality	Sample Number	Au g/t	Ag g/t	Cu ppm	Fe %	Hg ppb	Mo ppm	Pb ppm	S %	Sb ppm	Zn ppm	Occurrence of Ore
ES-3	ES-3-0	<0.01	<0.1	25	17.10	275	<1	5	4.75	2	36	Cyprus type semi-massive~disseminated pyrite・limonite
E-1	E-1-0	<0.01	<0.1	12,690	26.96	91	21	24	31.54	<1	187	Cyprus type semi-massive~disseminated pyrite・limonite・quartz・chalcopyrite
Kg-2	Kg-2-0	<0.01	<0.1	2,066	46.29	172	<1	19	2.48	<1	84	Cyprus type semi-massive limonite
KB-1	KB-1-0	<0.01	<0.1	1,950	55.85	155	19	<1	0.19	<1	103	boulder of Cyprus type massive hematite・limonite gossan
KB-3	KB-3-0	<0.01	<0.1	533	2.94	112	1	7	0.10	3	181	Cyprus type quartz・limonite vein
Po-1	Po-1-0	<0.01	<0.1	1,104	58.34	124	7	17	0.13	<1	181	boulder of Cyprus type masive hematite gossan
Po-2	Po-2-0	<0.01	<0.1	3,685	57.50	118	<1	12	0.19	<1	164	Cyprus type massive hematite・limonite gossan
Po-3	Po-3-0	<0.01	<0.1	3,997	55.58	99	138	1	0.03	<1	162	Cyprus type massive hematite・limonite gossan
SW-1	SW-1-0	<0.01	6.2	4,600	14.45	78	8	5	3.00	<1	232	Cyprus type lenticular~disseminated quartz・hematite・limonite・pyrite
SW-5	SW-5-0	<0.01	57.9	96	28.95	6,425	16	31	32.95	<1	48	Cyprus type lenticular~disseminated pyrite・limonite・quartz
SW-6	SW-6-0-1	<0.01	<0.1	837	2.55	32	2	8	1.67	<1	9,540	Cyprus type quartz・pyrite・limonite・sphalerite・chalcopyrite stockwork
SW-6	SW-6-0-2	<0.01	<0.1	2,129	4.23	45	9	6	2.99	<1	22,610	Cyprus type quartz・pyrite・limonite・sphalerite・chalcopyrite stockwork
ST-2	ST-2-0	<0.01	<0.1	142	8.12	68	<1	3	4.08	1	89	Cyprus type pyrite・limonite・quartz vein
ST-3	ST-3-0-1	<0.01	<0.1	1,542	23.20	45	<1	<1	8.51	<1	76	Cyprus type pyrite・limonite・quartz lens~stockwork
ST-3	ST-3-0-2	<0.01	<0.1	1,578	12.96	30	<1	<1	8.86	4	52	Cyprus type pyrite・limonite・quartz lens~stockwork
ST-4	ST-4-0	<0.01	<0.1	13	8.36	61	<1	5	2.90	5	50	Cyprus type quartz・limonite・pyrite vein
ST-5	ST-5-0	<0.01	<0.1	11,320	18.40	16	<1	7	9.15	<1	271	Cyprus type pyrite・limonite・quartz lens
ST-6	ST-6-0	<0.01	5.8	110,500	26.02	<10	<1	3	27.92	<1	324	Cyprus type pyrite・limonite・quartz・chalcopyrite・bornite vein
ST-9	ST-9-0	<0.01	0.8	9,726	11.86	<10	<1	5	4.21	5	71	Cyprus type pyrite・limonite・chalcopyrite・quartz stockwork
ST-10	ST-10-0	0.27	4.2	62,760	28.26	<10	<1	<1	29.59	<1	51	Cyprus type pyrite・quartz・limonite・chalcopyrite vein~lens
ST-11	ST-11-0-1	<0.01	<0.1	1,529	25.40	30	<1	<1	7.27	<1	61	Cyprus type limonite・pyrite・quartz vein
ST-11	ST-11-0-2	0.08	0.8	8,841	11.49	<10	<1	8	6.18	2	40	Cyprus type pyrite・limonite・chalcopyrite・quartz vein
ST-12	ST-12-0-1	<0.01	<0.1	927	17.67	22	<1	6	8.25	<1	28	Cyprus type pyrite・limonite・quartz・chalcopyrite stockwork~lens
ST-12	ST-12-0-2	<0.01	<0.1	45	18.30	<10	<1	8	7.16	<1	78	Cyprus type pyrite・limonite・quartz stockwork~lens
ST-13	ST-13-0	<0.01	<0.1	2,616	5.82	18	<1	3	2.13	6	44	Cyprus type quartz・limonite・pyrite・chalcopyrite・malachite stockwork
ST-15	ST-15-0	<0.01	<0.1	26,910	38.74	31	<1	9	7.52	<1	73	Cyprus type quartz・magnetite・limonite・pyrite・chalcopyrite・bornite・malachite stockwork
TE-1	TE-1-0	<0.01	<0.1	46,340	11.14	<10	5	4	10.88	<1	493	Cyprus type dissminated quartz・pyrite・chalcopyrite and vein
Tg-1	Tg-1-0-1	<0.01	<0.1	372	11.44	<10	<1	5	9.01	<1	33	Cyprus type pyrite・limonite lens and stockwork
Tg-1	Tg-1-0-2	<0.01	<0.1	2,679	10.61	<10	1	9	5.07	<1	24	Cyprus type pyrite・limonite lens and stockwork
UWS-2	UWS-2-0	<0.01	<0.1	2,142	6.73	22	<1	<1	2.79	7	196	Cyprus type quartz・pyrite・limonite・chalcopyrite stockwork
WS-1	WS-1-0	<0.01	<0.1	94,480	31.74	<10	36	16	35.03	9	5,799	drill core of Cyprus type massive pyrite・chalcopyrite ore
WS-3	WS-3-0	<0.01	<0.1	196	15.80	62	<1	10	6.65	6	118	Cyprus type lenticular pyrite・limonite
WS-4	WS-4-0	<0.01	<0.1	3,456	52.66	41	23	12	0.29	<1	65	boulder of Cyprus type massive hematite・limonite gossan
WS-5	WS-5-0	<0.01	<0.1	452	58.23	139	1	56	0.13	5	80	Cyprus type massive hematite・limonite gossan

Table II-2-9 List of Assay Result of Laterits Samples taken in Labuk Region

Locality	Sample Number	Au ppb	Co ppm	Cr ppm	Cu ppm	Fe %	Mn ppm	Ni ppm	Pt ppb
Bo-1	Bo-1-0-L	12	836	12,740	105	35.43	4,337	4,490	45
Ga-1	Ga-1-0-L	12	865	16,610	110	42.48	3,645	8,690	45
Ga-2	Ga-2-0-L	6	550	12,530	122	39.30	2,460	5,039	45
Kr-1	Kr-1-0-L	<6	1,136	22,150	184	45.86	5,032	8,056	60
NE-1	NE-1-0-L	2	309	6,553	163	18.76	3,824	4,253	20
Pm-1	Pm-1-0-L	6	405	21,870	84	48.86	1,729	4,003	60
Rk-1	Rk-1-0-L	4	148	14,590	53	42.35	1,015	2,804	40
SW-7	SW-7-0-L	4	76	1,470	144	13.40	1,544	897	5
TP-1	TP-1-0-L	<2	5,814	13,680	156	40.65	24,470	9,501	25
TE-2	TE-2-0-L	6	1,065	11,110	136	38.55	7,595	5,468	30
TE-3	TE-3-0-L	<6	850	15,670	132	39.55	4,028	6,438	60
UP-1	UP-1-0-L	<2	61	188	27	8.54	1,527	132	<5

2-5 Consideration

The conclusion obtained from the results of the investigation of the localities of mineral occurrence and the laboratory works on the samples of ore and rock is summarized below.

(1) Eleven localities of mineral occurrence of the massive, lenticular, veined, networked, and disseminated mineralized zone of Cyprus-type cupriferous iron sulfide, which consists mainly of pyrite, limonite, quartz, and chalcopyrite associated, in places, with minor amounts of bornite, chalcocite, covellite, malachite, sphalerite, and magnetite in places, in basalt and some dolerite of the ophiolite complex are found along the S. Telupid, situated about 6 kilometers west-northwest of Telupid, for a distance of about 160 meters.
The assay result of 14 ore samples taken at 11 localities reveals that the ore samples from 6 localities contain copper over 0.5% (0.88% to 11.05%).
Basalt and some dolerite in which the mineralized zone is embedded have been subjected to chloritization and partial epidotization.
The whole mineralized zone can be regarded as a copper-bearing network ore body which is relatively big in size with a length of about 155 meters in the direction of the northeast and a width of about 15 meters.

(2) Two outcrops (Po-2 and Po-3) and floats (Po-1) of massive gossan consisting of limonite and hematite are found around Kg. Porog to the north of Kg. Kiabau in the Bidu Bidu Hills area. Floats at the Po-1 locality can be nearly regarded as a outcrop.
These massive gossans contain 55.58 to 58.34% of iron and 0.11 to 0.40% of copper which still remain in gossans.
These massive gossans are considerably similar to those which are found at the surface of Cyprus-type massive cupriferous iron sulfide deposits of West Sualog and Kiabau in the Bidu Bidu Hills area in point of the megascopic observation, microscopic observation, and assay result.
Therefore, it seems that massive gossans at three localities have been probably formed by oxidation of Cyprus-type massive cupriferous iron sulfide body near the surface and it is possible that massive cupriferous iron sulfide body not oxidized is present under outcrop and its extension.

(3) The semi-massive, networked, and disseminated mineralized zone (Tg-1) of Cyprus-type cupriferous iron sulfide consisting of pyrite, limonite, quartz, and a

small amount of chalcopyrite, over 20 meters long and over 8 meters high, in metadolerite of the ophiolite complex are exposed along the S. Unsadan, a tributary of the S. Tungud, situated about 30 kilometers north-northwest of Telupid. One of two ore samples contains 0.27% of copper.

Considering that high Cu·Zn anomalies of the geochemical surveys by the use of stream sediment, conducted by the Malaysia-Germany exploration project for 1980 to 1984 and by the base metal exploration project of Geological Survey of Malaysia for 1986 to 1990, were detected in the upper basin of the S. Unsadan including the Tg-1 mineralized zone, there is a possibility that ore body of bigger size and of higher grade of copper than the Tg-1 mineralized zone may be present near the Tg-1 and that the mineralized zone of Cyprus-type cupriferous iron sulfide other than the Tg-1 may be found in the upper basin of the S. Unsadan.

(4) Veinlets, 2 to 5 centimeters wide, consisting of quartz, pyrite, and chalcopyrite and disseminated zone of pyrite in basalt of the ophiolite complex (TE-1) are found in a scattered pattern at the construction site of Forestry Training Institute of Telupid.

Ore sample taken from a veinlet in the mineralized zone contains 4.63% of copper. This mineralized zone is thought to be of Cyprus-type cupriferous iron sulfide and seems to be samller in size than those at Sungai Telupid and S. Tungud.

(5) The mineralized zone (E-1) of gravel-like, semi-massive, and disseminated Cyprus-type cupriferous iron sulfide consisting of pyrite, limonite, quartz, and a minor amount of chalcopyrite in pillow basalt of the ophiolite complex is found at the roadside, situated about 24 kilometers north-northwest of Telupid, in the upper basin of the S. Ensuan, a tributary of the S. Labuk. The whole mineralized zone is lenticular in shape with a length of 2.2 meters and a maximum width of 1.5 meters.

The sample taken from a gravel-like ore, 15 centimeters long and 10 centimeters wide, contains 1.27% of copper.

The mineralization at the E-1 locality seems to be weak, judging from that there is only one small lenticular mineralized zone.

(6) Each veinlet within network of Cyprus-type cupriferous iron sulfide found in Bidu Bidu Hills and Telupid areas shows no definite direction and fractures of all the direction have been mineralized.

(7) Basalt and some dolerite of the ophiolite complex accompanied by the mineralized zone have been subjected to chloloritization, epidotization, and partial silicification and are rich in quartz network in general.

(8) The mineralized zone of Cyprus-type cupriferous iron sulfide found in the Bidu Bidu Hills and Telupid areas seems to be present in the area where basalt, dolerite, gabbro, and ultrabasic rock constituting the ophiolite complex are distributed complicatedly due to many faults and seems to be embedded in basalt and some dolerite associated with gabbro, especially, in the area between relatively big ultrabasic rock bodies within the above area.
It appears that the Bidu Bidu Hills area, Bt. Luminintong area, and the area between Telupid and S. Karang have the above geologic conditions.

(9) It is said that network ore body of Cyprus-type cupriferous iron sulfide accompanies overlying massive ore body in general.
However, there is a possibility that each ore body may exist individually or both the ore bodies may occur together at the same depth in the area, where faults dominate and geology is complicated, in the Labuk region.

(10)The assay result of the samples of laterite formed by weathering of ultrabasic rock reveals that the majority of the samples contain 1.11 to 2.22% of chromium and 0.40 to 0.95% of nickel and that laterite rich in chromium contains much nickel in general.

(11)The chemical analyses of 11 samples of basalt and 8 samples of dolerite of the ophiolite complex taken in the Bidu Bidu Hills and Telupid areas have been plotted on the several diagrams for the petrological study.
The result obtained from the TiO_2-FeO*/MgO diagram reveals that all the rock samples belong to MORB (Mid-ocean ridge basalt) series (FeO*: calculated as total FeO from the analyses of FeO and Fe_2O_3).

Part III Conclusion and Recommendation

PART III CONCLUSION AND RECOMMENDATION

CHAPTER 1 CONCLUSION

It seems that base metal deposit with possibility of discovery in the future in the Kinabalu and Labuk regions surveyed in 1992 may be gold deposit in Bt. Tampang area of Kinabalu region and Cyprus-type cupriferous iron sulfide deposits in and around Sungai Telupid, Kg. Porog, and S. Tungud mineralized zones in the Labuk region.
The mineralized zone of veinlets, network, and dissemination, consisting of quartz with minor amounts of pyrite and limonite, embedded in acidic to intermediate volcanic and pyroclastic rocks subjected to hydrothermal alteration, is found at the western and southern foots of Bt. Tampang.
This gold-bearing mineralized zone seems to correspond to the upper part of epithermal gold deposit accompanying intermediate to weak alkaline hydrothermal fluid related to the volcanic activity which took place probably during Miocene to Pliocene time, considering that some veinlets in the mineralized zone contain gold (2.68 g/t), antimony (0.13%), and mercury (22.05 ppm, 22.45 ppm) and the alteration mineral assemblage of hydrothermally altered rock consists mainly of quartz, sericite, kaolinite, and chlorite accompanied, in places, by some potash felspar and smectite and that homogenization temperature of fluid inclusions in quartz taken from quartz veinlets ranges from 218° to 259°C except for 278° to 284°C of one sample.
Therefore, there is a possibility that gold-bearing quartz vein of the bonanza-type or vein-type may be present under this mineralized zone.
It is possible that such a gold-bearing mineralized zone may be found at the eastern and northern foots and the hillside of Bt. Tampang besides the western and southern foots.
It seems that a hill ranging to the west-northwest of Bt. Tampang, Bt. Kotud, Bt. Tambiau, Bt. Kalarakan, and Bt. Tu'us to the north of Bt. Tampang may be formed of acidic to intermediate volcanic and pyroclastic rocks. If so, there is also a possibility that gold-pyrite-quartz bearing mineralized zone, accompanied by hydrothermal alteration zone, as found at the foot of Bt. Tampang may be present at the foots and hillsides of these hills.

The mineralized zone of Cyprus-type cupriferous iron sulfide found in the Bidu Bidu Hills and Telupid areas seems to be present in the area where basalt, dolerite, gabbro, and ultrabasic rock constituting the ophiolite complex are distributed

complicatedly due to many faults and seems to be embedded in basalt and some dolerite associated with gabbro, especially, in the area between relatively big ultrabasic rock bodies within the above area.

It appears that the Bidu Bidu Hills area, Bt. Luminintong area, and the area between Telupid and S. Karang have the above geologic conditions.

It is said that network ore body of Cyprus-type cupriferous iron sulfide accompanies overlying massive ore body in general. However, there is a possibility that eaach ore body may exist individually or both the ore bodies may occur together at the same depth in the area, where faults dominate and geology is complicated, in the Labuk region.

The promising mineralized zones of Cyprus-type cupriferous iron sulfide except known ore deposits and mineral occurrences in the Bidu Bidu Hills area are the Sungai Telupid mineralized zone, Kg. Porog mineralized zone, and S. Tungud mineralized zone, judging from the above geological condition and the result of the survey in 1992.

The Sungai Telupid mineralized zone which is embedded in basalt and some dolerite found along the Sungai Telupid consists mainly of pyrite, limonite, quartz and chalcopyrite accompanied, in places, by bornite, chalcocite, covellite, malachite, sphalerite, and magnetite. This mineralized zone is semi-massive, lenicular, veined, networked, and disseminated in occurrence at each locality of mineral occurrence, and the whole mineralized zone can be regarded as a network ore body with a length of about 155 meters in the direction of the northeast and a width of about 15 meters.

In case this mineralized zone is regarded as a network ore body, network body will be poor in ore and of low copper grade. However, there is a possibility that network ore body or massive ore body of high copper grade may be emplaced near this mineralized zone.

Kg. Porog mineralized zone is composed of two outcrops and floats, which can be nearly regarded as a outcrop, of massive gossan consisting of limonite and hematite. These massive gossans are considerably similar to those which are found at the surface of Cyprus-type massive cupriferous iron sulfide deposits of West Sualog and Kiabau in the Bidu Bidu Hills area in point of megascopic observation, microscopic observation, and assay result.

Therefore, it seems that massive gossans at three localities of mineral occurrence have been probably formed by oxidation of Cyprus-type massive cupriferous sulfide body near the surface and there is a possibility that massive cupriferous iron sulfide body not oxidized may be emplaced under outcrop and its extension.

The S. Tungud mineralized zone consisting of pyrite, quartz, and a minor amount of

chalcopyrite, over 20 meters long and over 8 meters high, is found along the S. Unsadan, a tributary of the S. Tungud, in the Bt. Luminintong area. This mineralized zone is semi-massive, networked, and disseminated in occurrence, but the whole mineralized zone is nearly semi-massive and poor in copper.
Considering that high copper and zinc anomalies of geochemical surveys by the use of stream sediment, carried out by the Malaysia-Germany exploration project for 1980 to 1984 and by the base metal exploration project of Geological Survey of Malaysia for 1986 to 1990, were detected in the upper basin of the S. Unsadan including this Tg-1 locality of mineral occurrence, there is a possibility that ore body of bigger size and of higher grade of copper than the Tg-1 mineralized zone may be emplaced near the Tg-1 locality and that the mineralized zone of Cyprus-type cupriferous iron sulfide other than the Tg-1 may be present in the upper basin of the S. Unsadan.

In addition to the above, the veined hydrothermal alteration zones accompanied, in places, by some limonite and quartz are found along many parallel joints in quartz monzonite porphyry around Bt. Luminantai. Hydrothermal alteration veins are narrow in width (1 to 30 centimeters) and form network as a whole.
There is a possibility that these hydrothermal alteration veins may correspond to the SCC alteration zone (sericite-clay-chlorite) accompanying the upper part of porphyry copper deposit, judging from the results of assay of limonite·quartz veinlet accompanying hydrothermal alteration vein, X-ray diffraction examination of hydrothermal alteration vein, and measurement of homogenization temperature of fluid inclusion in quartz taken from limonite·quartz veinlet. However, considering that ore samples for assay, clay samples for X-ray diffraction, and quartz sample for measurement of homogenization temperature are short of the number and that quartz monzonite porphyry between hydrothermal alteration veins has not been subjected to hydrothermal alteration, a definite conclusion about the above must be reserved.
Therefore, it is necessary to conduct further detailed geological mapping, assay of ore sample, X-ray diffraction examination, and measurement of homogenization temperature and salinity of fluid inclusion in quartz in order to clarify whether these hydrothermal alteration veins accompany the upper part of porphyry copper deposit or not.

CHAPTER 2 RECOMMENDATION FOR PHASE IV SURVEY

As mentioned in the above "Chapter 1 Conclusion", it seems that base metal deposit with possibility of discovery in the future in the Kinabalu and Labuk regions surveyed in 1992 may be gold deposit in Bt. Tampang area of Kinabalu region and Cyprus-type cupriferous iron sulfide deposits in and around Sungai Telupid, Kg. Porog, and S. Tungud mineralized zones in the Labuk region.
Therefore, the following follow-up works for the above promising mineralized zones are recommended.

1. Bt. Tampang mineralized zone

   (1) Detailed geological mapping; K-Ar dating, chemical analysis, and microscopic observation of host rock; systematic sampling, assay, and microscopic observation of ore; X-ray diffraction examination of hydrothermally altered rock; measurement of homogenization temperature and salinity of fluid inclusion in quartz taken from quartz veinlets; and geolchemical survey by the use of soil at the foot and hillside of Bt. Tampang.

   (2) The same follow-up works as the above, except for geochemical survey, at the foots and hillsides of a hill ranging to the west-northwest of Bt. Tampang, Bt. Kotud, Bt. Tambiau, Bt. Tu'us, and Bt. Kalarakan to the north of Bt. Tampang.

2. Sungai Telupid mineralized zone

   Detailed geological mapping; K-Ar dating, chemical analysis, and microscopic observation of host rock; systematic sampling, assay, and microscopic observation of ore; and geochemical survey by the use of soil in and around the mineralized zone.

3. S. Porog mineralized zone

   Detailed geological mapping; K-Ar dating, chemical analysis, and microscopic observation of host rock; systematic sampling, assay, and microscopic observation of ore; and geochemical survey by the use of soil at and around outcrops.

4. S. Tungud mineralized zone

Detailed geological mapping; K-Ar dating, chemical analysis, and microscopic observation of host rock; systematic sampling, assay, and microscopic observation of ore; and geochemical survey by the use of soil in and around mineralized zone.

Next, the detailed geological mapping; chemical analysis, microscopic observation, and X-ray diffraction examination of hydrothermal alteration vein; assay and microscopic observation of limonite·quartz veinlets in hydrothermal alteration veins; and measurement of homogenization and salinity of fluid inclusion in quartz taken from limonite·quartz veinlets are recommended in order to clarify whether hydrothermal alteration veins in quartz monzonite porphyry around Bt. Luminantai accompany the upper part of porphyry copper deposit or not.

REFERENCES

Collenette, P., (1954): Geological Reconnaissance of the Kinabalu Area. Annual report of the Geological Survey Department for 1954, British Territories in Borneo, P.111-123.

Collenette, P., (1958): The geology and mineral resources of the Jesselton-Kinabalu area, North Borneo. Memoir 6, Geological Survey Department, British Territories in Borneo.

Collenette, P., (1963): A phisiographic classification for North Borneo. Jour. of Tropical Geography, V.17, p.28 ~ 33.

Fitch, F.H., (1958): The geology and mineral resources of the Sandakan area and parts of the Kinabatangan and Labuk valleys, North Borneo. Geological Survey Department, British Territories in Borneo, P.9-25.

Hayba, D.O., Bethke, P.M., Heald, P. and Foley, N.K., (1986): Geologic, mineralogic, and geochemical characteristics of volcanic-hosted epithermal precious-metal deposits. Reviews in Econ. Geol., V.2, P.129-167.

Heald, P., Foley, N.K. and Hayba, D.O., (1987): Comparative anatomy of volcanic-hosted epithermal deposits; acid-sulfate and adularia-sericite types. Econ. Geol., V.82, P.1-26.

Hedenquist, J.W., (1987): Volcanic related hydrothermal systems in the Circum-Pacific basin and their potential for mineralization. Mining Geol., V.37, P.347-364 (in Japanese with English abstract).

Izawa, E. and Urashima, Y., (1988): Quaternary gold mineralization and its geologic environments in Kyushu, Japan. Econ. Geol. Mono. 6, The geology of gold deposits, P.233-240.

Jacobson, G., (1970): Gunung Kinabalu area, Sabah, Malaysia. Report 8, Geological Survey of Malaysia, P.1-3.

Lee, D.T.C., (1985): Regional geology, Sabah. Annual report for 1985, Geological

Survey of Malaysia, P.122-130.

Nagano, K., Takenouchi, S., Imai, H. and Shoji, T., (1977): Fluid inclusion study of the Mamut porphyry copper deposit, Sabah, Malaysia. Mining Geol., V.27, P.201-212.

Newton-Smith, J., (1967): Bidu Bidu Hills area, Sabah, East Malaysia. Report 4, Geological Survey, Borneo Region, Malaysia, P.1-6.

Shikazono, N., Nakata, M. and Shimizu, M., (1990): Geochemical, mineralogic and geologic characteristics of Se- and Te-bearing epithermal gold deposits in Japan. Mining Geol., V.40, P.337-352.

Sillitoe, R.H., (1973): The tops and bottoms of porphyry copper deposits. Econ. Geol., V.68, P.799-815.

Sillitoe, R.H., (1988): Gold deposits in western Pacific island arcs; the magmatic connection. Econ. Geol., Mono. 6, The geology of gold deposits, P.274-288.

Takenouchi, S., (1981): Fluid inclusion studies of several Philippine porphyry copper deposits. Rept. Geol. Surv. Japan, No.261, P.149-167.

Takenouchi, S., (1981): Fluid inclusion studies of Tertiary gold deposits. Mining Geol., Mono. 10, P.247-258 (in Japanese with English abstract).

Takenouchi, S., (1983): Fluid inclusion study of the Nansatsu-type gold deposits. Mining Geol., V.33, P.237-245 (in Japanese with English abstract).

Yan, A.S.W., (1987): Follow-up geochemical exploration for base metals in the Bukit Luminintong area, Labuk Valley, Sabah. Anuual report for 1987, Geological Survey of Malaysia, P.375-387.

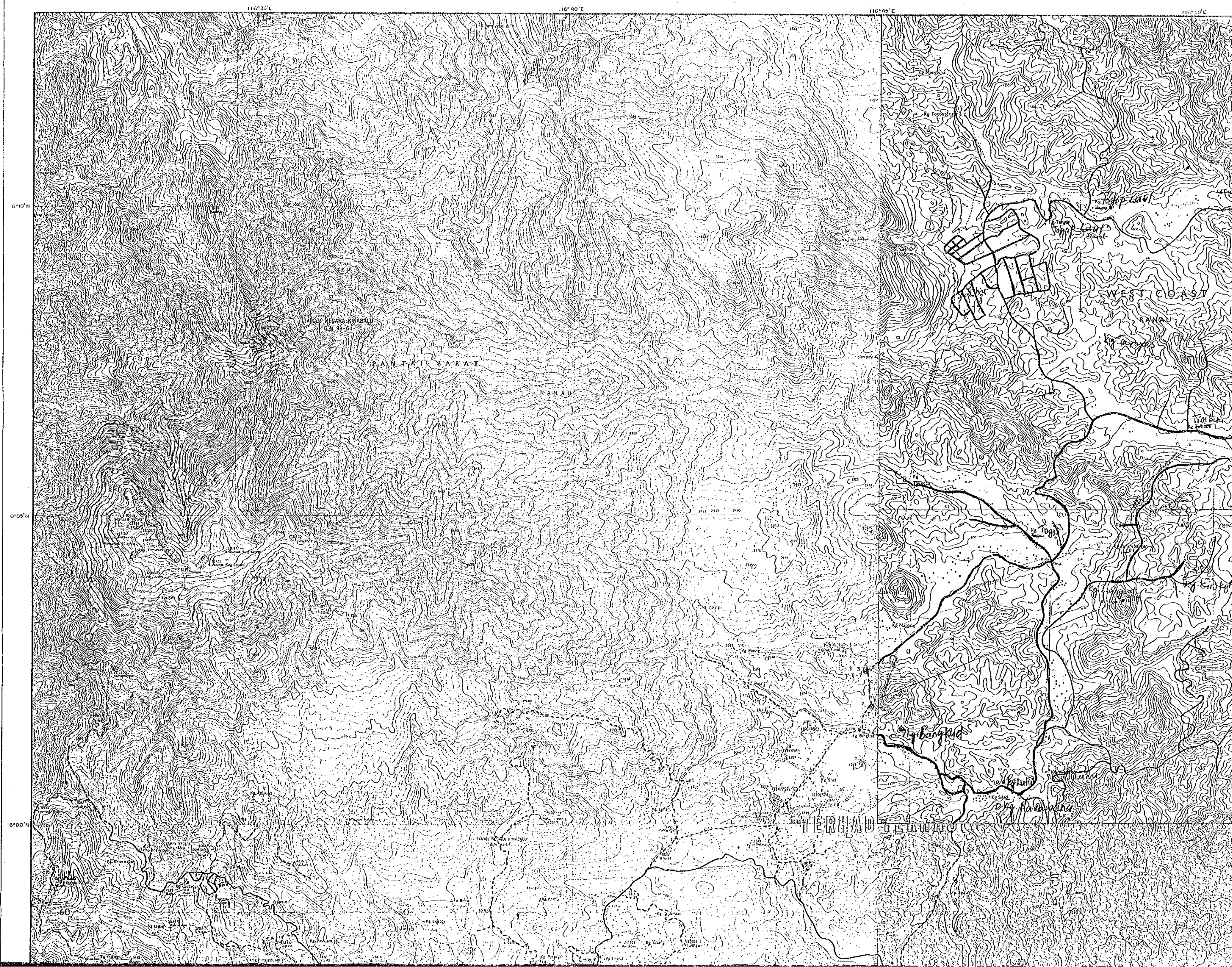
116°35'E
116°40'E
116°45'E
116°50'E
6°10'N
6°05'N
6°00'N
PANTAI BARAT
RANAU
WEST COAST
RANAU
Kg Togop Laut
Kg Togi
Kg Naisog
Kg Silad
T-3
T-7
T-1
T-10
Lu-3
Lu-2
TERHAD